



Norwegian University of
Science and Technology

Theoretical study of Mechanical Stability of charcoal from biomass resources

Håkon Bergflødt Narjord

Master of Energy and Environmental Engineering

Submission date: July 2017

Supervisor: Terese Løvås, EPT

Norwegian University of Science and Technology
Department of Energy and Process Engineering

Agreement concerning MSc theses and supervision

This Agreement confirms that the topic for the MSc thesis approved, the supervisory issues are agreed and the parties to this Agreement (student, supervisor and department) understand and accept the guidelines for MSc theses. This Agreement is also subject to Norwegian law, the examination regulations at NTNU, the supplementary provisions and the regulations for the MSc Engineering Education programme.

1. Personal information

Family name, first name: Narjord, Håkon Bergflødt	Date of birth May 22, 1988
Email address haakonbn@stud.ntnu.no	Phone 41568917

2. Department and programme of study

Faculty Faculty of Information Technology and Electrical Engineering
Department Department of Electric Power Engineering
Programme of study Master of Energy and Environmental Engineering

3. Duration of agreement

Starting date January 31, 2017	Submission deadline* June 27, 2017
If part-time study is approved, state percentage:	

* Including 1 week extra for Easter

All supervision must be completed within the duration of the agreement.

4. Thesis working title

Theoretical study of Mechanical Stability of charcoal from biomass resources

5. Supervision

Supervisor Terese Løvås

Standardized supervision time is **25 hours** for 30 credits (siv.ing) and **50 hours** for 60 credits (MST) theses.

6. Thematic description

In the silicon and ferrosilicon production process a 35% reduction in overall energy consumption and close to zero CO₂ emissions by replacing all fossil reduction material (mainly coal and coke) with a renewable source; charcoal from biomass. When handled, transported, loaded, and charged into the furnace in the silicon production process charcoal produces significant amounts of small particles; so-called charcoal fines, or just fines. The fines do not contribute to the performance of the silicon production process and typically burn on top of the charge in the oven. Hence, if the amount of fines could be reduced this could contribute significantly to the process economy when using charcoal in the silicon production process. Biochar has also been discussed as a replacement for fossil coal in other metallurgical processes, such as cast iron production in a cupola furnace or iron ore reduction in a blast furnace. As in silicon and ferrosilicon production, the processes require the carbon carrier to have specific properties. A certain mechanical strength is necessary to provide structural stability in the furnace. This master thesis assignment will focus on the mechanical properties of biochar, produced via pyrolysis of different biomasses. The thesis will investigate if and how mechanical properties such as grindability, abrasion resistance and compressive strength can be correlated to the properties of biochar (proximate and ultimate analysis, particle size, etc.) and hence to the production conditions. A comprehensive literature screening aims to analyse the work that has already been done in this field. Pelletization and briquetting will also be considered as an additional step to alter mechanical properties. In addition, the results obtained during a project work (on the mechanical stability of charcoal)

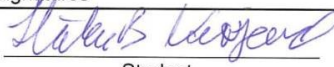
will be used to develop a mathematical correlation between the amount of fines and the production conditions of the biochar.

7. Other Agreements

Supplementary agreement	Not applicable
Approval required (REK, NSD)	Not applicable
Risk assessment (HES) done	Not applicable

Appendix (list)

8. Signatures

Conditions	Date	Signatures
I have read and accept the guidelines for MSc theses		 Student
I take the responsibility for the supervision of the student in accordance with the guidelines or MSc theses		_____ Supervisor
Department/Faculty approves the plan for the MSc thesis		_____ Department/Faculty

Abstract

There is a large potential for lowering CO₂ emissions from the metallurgical industry if carbon neutral bio based reductants could replace fossil coke. The inferior mechanical stability of bio based charcoal is one of the most important impediments to this.

This study reviews the mechanical stability of bio based charcoal and torrefied biomass. Data was compiled from ten different studies. Of these, seven tested the friability of charcoal (quantified by means of tumbler drum), and three examined the grindability of torrefied biomass, expressed by the Hardgrove Grindability Index (HGI). The data were compared, discussed, and analysed using statistical tools such as analysis of variance and principal component analysis.

The findings suggest that *Eucalyptus grandis* charcoal is less friable when the wood is drier and/or younger, while peak carbonization temperature has a minor effect. The friability was higher for carbonization temperature 500°C than for both 300°C and 700°. The fixed carbon content was found to be a poor indicator of the friability of charcoal, but a better indicator of the HGI of torrefied biomass. The best correlation with HGI was found to be the gravimetric yield, and torrefied *Eucalyptus* sp. was the least grindable, and a sample of torrefied softwood the most grindable, in relation to their gravimetric yields.

Sammendrag

Det er et stort potensiale for å redusere CO₂-utslipp fra den metallurgiske industrien hvis bio-baserte reduktanter kunne erstatte koks. Kanskje det største hinderet for dette, er at trekull er at trekull har dårligere mekaniske egenskaper enn koks.

I dette studiet undersøkes de mekaniske egenskapene til trekull og torrefiert biomasse. Data er hentet fra ti forskjellige kilder. Syv av disse omhandler testing av skjørheten trekull, eller dets tendens til å smuldre, som er testet i en roterende trommel. De tre siste inneholder mekanisk testing av torrefiert biomasse, hvis resultater er uttrykt ved Hardgrove Grindability Index (HGI). Dataen ble sammenlignet, diskutert og analysert ved hjelp av statistiske verktøy som analysis of variance and principal component analysis, med flere.

Resultatene indikerer at trekull fra *Eucalyptus grandis* som har lavere vanninnhold og/eller er fra yngre trær, er mindre skjørt, mens høyeste pyrolyse-temperatur har mindre effekt. Trekull behandlet ved 500°C var skjørere enn det som var behandlet ved både 300°C og 700°C. Innholdet av fast karbon er en dårlig indikator for skjørhet for trekull, men en bedre indikator for HGI-verdi for torrefiert biomasse. HGI korrelerte best med masse-tap blant de målte verdiene. I forhold til masse-tapet, hadde *Eucalyptus* sp. lavest HGI, og en prøve med bartrær hadde den høyeste.

Contents

Abstract.....	1
Sammendrag	2
Contents	3
List of figures	5
List of tables	7
List of abbreviations and nomenclature	8
Introduction	9
Production of charcoal	10
Charcoal production today	11
Historical and current use of charcoal	12
Charcoal as fuel.....	12
Soil amendment.....	13
Metallurgy.....	14
Reintroducing charcoal in metallurgy.....	15
Wood structure and composition	17
Structural components	17
Extractives.....	19
Ash	20
Moisture content.....	20
Softwood structure	21
Hardwood structure	22
Sapwood and heartwood	23
Pyrolysis of wood	25

Primary and secondary reactions	27
Proximate analysis.....	28
Maximum fixed carbon yield	28
Feedstock composition and char yield	29
Temperature	31
Particle size, pressure and flow rate.....	32
Measurement of density and porosity	32
Mechanical strength of charcoal	35
Compressive strength	36
Data analysis	40
Friability tumbler tests	40
Carbonization temperature	43
Tree age	46
Wood moisture content	47
Model for friability.....	50
Principal component analysis friability	53
Friability varying with tree diameter	57
The five smaller studies.....	59
Stadardized plots of friability.....	61
Comparative plots data	62
Grindability.....	67
Principal component analysis grindability	70
Plots of HGI and strongest correlates	74
Conclusions	79
References.....	81

List of figures

Figure 1: Cellulose represented by two linked glucose molecules (Kataki et al., 2015)	17
Figure 2: Hemicellulose, represented by different linked monomers (Kataki et al., 2015)	18
Figure 3: A sample lignin (Kataki et al., 2015).....	18
Figure 4: Softwood cellular structure (Schweingruber, 1966).....	21
Figure 5: Hardwood structure (Schweingruber, 1966)	22
Figure 6: Typical mass loss (a) and rate of mass loss (b) as a function of temperature for cellulose, lignin and hemicellulose (represented by xylan).(Jin et al., 2013).....	26
Figure 7: Carbonization of beech (Schenkel, 1999)	31
Figure 8: Pyrolysis front (United States Department of Agriculture, 2010)	32
Figure 9: <i>Salvadora oleoides</i> , treated at 200°C and compressed parallel to fibres (Lancelotti et al., 2010).....	36
Figure 10: Compressive strength (crushing strength)(Kumar et al., 1999)	37
Figure 11: Gravimetric yield (a) and fixed carbon content (b) for the carbonization temperature levels, n=9 for all boxes.....	43
Figure 12: Friability (a) and apparent density (b) for the carbonization temperature levels, n=9 for all boxes.....	44
Figure 13: Apparent density and friability with standard deviations for the carbonization temperature levels.....	44
Figure 14: Gravimetric yield (a) and fixed carbon content (b) for the tree age levels, n=9 for all boxes.....	46
Figure 15: Friability (a) and fixed apparent density (b) for the tree age levels, n=9 for all boxes.....	46
Figure 16: Gravimetric yield (a) and fixed carbon content (b) for the wood water content levels, n=9 for all boxes.....	48
Figure 17: Friability (a) and fixed apparent density (b) for the wood water content levels, n=9 for all boxes.....	48

Figure 18: Fixed carbon content as a function of temperature. The dotted lines are temperature and corresponding fixed carbon content at maximum friability.	52
Figure 19: Friability vs fixed carbon content.....	52
Figure 20: Biplot.....	55
Figure 21: Friability varying with carbonization temperature and tree diameter.	57
Figure 22: Standardized friability versus standardized fixed carbon content, apparent density, gravimetric yield and ash content.	62
Figure 23: Friability vs fixed carbon content.....	63
Figure 24: Friability vs apparent density.....	64
Figure 25: Friability vs gravimetric yield	65
Figure 26: Friability vs ash content	65
Figure 27: Biplot.....	72
Figure 28: HGI for three ranges of RT/PS. For boxes left to right: n=10, n=8, n=9.....	73
Figure 29: HGI vs temperature	75
Figure 30: Deviation temperature regression line for each biomass type. Boxes from left to right: n=8, n=3,n=3,n=4,n=3, n=6.	75
Figure 31: HGI vs gravimetric yield	76
Figure 32: Deviation from gravimetric yield regression line for each biomass type. Boxes from left to right: n=8, n=3,n=3,n=4,n=3, n=6.	76
Figure 33: HGI vs fixed carbon content.....	77
Figure 34: Deviation from fixed carbon content regression line for each biomass type. Boxes from left to right: n=8, n=3,n=3,n=4,n=3, n=6.	77

List of tables

Table 1: Pyrolysis types (Ronsse et al., 2015).....	25
Table 2: Charcoal and coke requirements (Rousset et al., 2011).....	38
Table 3: Compressive strength of some charcoals	39
Table 4: Wood and charcoal properties (de Oliveira et al., 1982a).....	42
Table 5: Output from generation of linear model in R.	50
Table 6: Pearson correlation matrix.	53
Table 7: Importance of components.....	54
Table 8: Loadings of variables on principal components.....	54
Table 9: Friability standard applied, and cut off size for fines (* Size reduction measured according to NBR 7416/84 of ABNT, which involves several cut off sizes for fines)	59
Table 10: Charcoal properties	60
Table 11: Torrefied biomass properties.....	68
Table 12: Pearson correlation matrix	70
Table 13: Importance of principal components.....	70
Table 14: Loadings of variables on principal components.....	71

List of abbreviations and nomenclature

		Units
HGI	Hardgrove Grindability Index	
Age	tree age	years
Water	wood moisture content	%
Temp	highest treatment temperature	°C
db	dry basis	
wb	wet basis	
FC	fixed carbon content	%
Ash	ash content	%
VM	volatile matter content	%
GY	gravimetric yield	%
D	apparent density	[g cm ⁻³]
TD	true density	[g cm ⁻³]
P	porosity	
Fri	friability	%
HR	heating rate	°C min ⁻¹
RT	residence time	minutes
PS	particle size	mm
ABNT	Associação Brasileira de Normas Técnicas	
ANOVA	Analysis of variance	
PCA	Principal component analysis	

Introduction

The predominant reducing agent used in metallurgy today is fossil coal and coke. According to an IPCC report from 2005, the iron and steel industry, which is the largest among the metallurgical industries, account for about 4.8% of the global CO₂ emissions from large industrial stationary sources (IPCC, 2005). Bio based reductants can be CO₂-neutral, as the carbon they contain is fixed from the atmosphere via photosynthesis by the growing plant, and released as CO₂ after consumption. Although properties like high carbon content, low ash content and high reactivity make charcoal an excellent reducing agent, some of its mechanical properties make direct substitution of coke by lump charcoal challenging. Charcoal is more friable and less resistant to compressive stress. A better understanding of how these mechanical properties relate to the wood precursor, pyrolysis conditions and other properties of the charcoal, can help charcoal manufacturers produce a more durable charcoal fit to replace coke in more cases than it currently does. The parameters which can be directly adjusted during the production, like temperature, heating rate, feedstock species and feedstock pre-treatment are of interest, from a practical standpoint. Particular attention is also paid to the relationship between friability and fixed carbon content, since the fixed carbon content is considered decisive in the determination of charcoal quality in a metallurgical context (Antal and Grønli, 2003).

The thesis starts with a summary of the history of the production and use of charcoal. Then follows a section on the structure and composition of wood, and on its pyrolysis. In the data analysis section, data from mechanical tests on charcoal and torrefied biomass has been gathered from the literature. The first a study with friability testing of charcoal made from *Eucalyptus grandis*, is from a comprehensive collection of studies on charcoal performed by de Oliveira et al., (1982). Six smaller studies performing similar mechanical testing are then analysed, discussed and compared to the first (de Assis, 2007; Coutinho and Ferraz, 1988; Gomes da Silva et al., 2007; Lana, 2012; Noumi et al., 2014; da Silva et al., 2014). The final data analysed is on grindability testing done on torrefied biomass from three separate studies (Bridgeman et al., 2010; Ohliger et al., 2013; Raimie H. H. et al., 2013). All of the data is analysed using various statistical tools, and discussed. Finally, some conclusions are drawn.

Production of charcoal

The traditional way of producing charcoal is lighting a fire of closely stacked split wood or branches to which the air supply can be controlled. At the right time, the air supply is cut off, and the fire is left in an oxygen deprived smoulder, which is maintained by exothermic reactions. Once complete carbonization is achieved, the charcoal can be gathered several hours or days after the process was initiated. The earliest methods to achieve this are charcoal pits or mound kilns. These are temporary kilns operating in batch mode often with the sole purpose of producing charcoal disregarding the by-products. Being simple and inexpensive, they are still applied today, especially in the developing world. In the case of pits, a hole is dug, filled with wood and lit with a cover on top to control the air supply. The mound kiln is essentially an above ground version of the charcoal pit where digging a hole is not practical because of rocky, hard soil, water table close to the surface, or some other reason. The charcoal pits and mound kilns have taken a range of different sizes and shapes through history with pits ranging from around 1 m³ to 30 m³ or larger. There is necessarily some combustion in these kinds of installations, and they require continuous tending to optimize the air supply. Because of this the charcoal yield is generally low, but they can produce charcoal of decent quality depending on the feedstock and the sophistication of the process. The mound kiln was improved upon by constructing more permanent structures made of stone, brick and eventually metal allowing for reuse of the installation, and more precise control of the process.

Variations of the simple pyrolysis installations mentioned also have a long history of use where charcoal was not the most desired product. If built in the shape of a funnel, the mound kiln allows the collection of the tarry runoff from underneath the kiln. The use of wood derived tars, oils and resins were used in mummification in ancient Egypt (Abdel-Maksoud and El-Amin, 2011), and tar has been found connecting arrowheads to arrows thousands of years old (Emrich, 1985). Funnel shaped kilns, believed to have been used for pine tar production, have been found in Sweden and dated to 240-540 AD, making them the oldest of their kind known in Europe (Hjulström et al., 2006). Pine tar has been particularly valuable to

ship builders who have used it to caulk the hull of ships, and to waterproof sails and rope. In modern times, synthetic materials have replaced tar in many of its traditional applications, and the gaseous and liquid products of biomass pyrolysis are made use of in other ways.

As the charcoal making process became more sophisticated, attention was paid to improving the energy balance. Instead of venting the vaporized volatiles to the atmosphere, they were condensed and refined into various valuable chemicals, or burned. The combustion of these gases could be used to generate electricity, or to become a heat source to the pyrolysis itself in retort kilns.

After world war two, a process known as rapid pyrolysis became commercially proved. The operation could be continuous rather than batch-based, and allowed for smaller sized feedstock (Emrich, 1985). The feedstock was now no longer limited to split dry wood, but could be any kind of biomass like sawdust, corn husks or other agricultural or industrial waste. The rapid pyrolysis process increases the liquid and gas yield at the expense of the solid yield, and is thus well suited for production of bio oils and associated products. The resulting char powder, although unfit for metallurgical uses in most cases, can be used as biochar or briquetted.

Charcoal production today

Modern industrial production of wood charcoal is done with internal heating, external heating or recirculation of combustible gases into the pyrolysis chamber (Antal and Grønli, 2003). The Missouri kiln and Brazilian beehive kiln are two much used internal heating kilns operating in batch mode where the heat initiating the pyrolysis process is the partial combustion of the feedstock in the pyrolysis chamber. In the more sophisticated Van Marion Retort, no combustion takes place in the two separated pyrolysis chambers. One is loaded with wood and pyrolysis is initiated. Once the pyrolysis in this chamber enters the exothermic self-sustaining phase, the combustible off gases are led into a combustor that heats and initiates pyrolysis in the second chamber. When the wood in the first chamber is carbonized, it is swapped for one with fresh wood, and the cycle continues, the second chamber now heating the first.

An example of the third method is the Degussa (Reichert) process. Also a batch based process, the condensable gases are removed from the off gasses for refining, and the remaining gases are then fed back into the retort.

Historical and current use of charcoal

Charcoal made from wood may be one of the first substances synthesised by humans. The earliest known applications are prehistoric cave paintings made with charcoal in the Chauvet Cave in southern France. They have been, estimated to be about 31,000 years old (Bard, 2001). Throughout the millennia many other applications of charcoal and its associated by-products have been documented.

Charcoal as fuel

As a fuel used for cooking or heating, charcoal has several properties, which made it desirable. By charring organic matter, i.e. converting it to charcoal, it becomes highly resistant to chemical and biological degradation allowing it to be stored almost indefinitely in conditions where the uncharred feedstock, like wood, would rot (Lehmann and Joseph, 2015).

When wood is converted to charcoal in traditional charcoal production, it loses mass and its size is normally slightly reduced. Since some of the weight loss is the volatilization of combustible compounds, like tar, the absolute energy content [kJ] of a given piece of wood is reduced during carbonization. However, the mass loss is normally much greater than the loss of absolute energy content, resulting in approximately a doubling of the specific heating value [kJ/kg] in the charcoal compared to the wood feedstock, of course depending on the feedstock and pyrolysis conditions (Keita, 1987). This makes for more efficient transportation if the weight of the fuel is a limiting factor. The heating value of wood can vary greatly depending on species, but the variance decreases after carbonisation. The “three-stone

stove” is among the simplest of food preparation installations. It is a pan or a pot above a fire supported by three stones or bricks, which is still common in certain developing countries. The efficiency of this installation is here defined as the potential thermal energy in the fuel transferred to its intended target, i.e. the pot or pan. Wood fuel used in this setting is not ideal as the heat transfer to the food by convection is predominant, resulting in an efficiency of about 8% (Keita, 1987). This is because of the volatiles in the wood evaporate and combust in the visible flames. This spread of the combustion and any moisture in the wood, result in a lower temperature fire, which in turn may result in incomplete combustion producing soot. During carbonisation, most of the volatile compounds are removed from the wood leaving a more homogenous solid relatively enriched in carbon. Charcoal provides a more stable, higher temperature fire with less visible flames and smoke, which makes them preferable to wood fires in densely populated areas, and for cooking inside. In a three-stone-stove fuelled with charcoal, the radiative heat transfer is greater, compared to a wood fire, resulting in an efficiency of about 28% (Keita, 1987). The loss in absolute heating value of wood through carbonisation is less than this gain in efficiency. In other words, in a three-stone stove, a given amount of wood can provide a warmer soup, if carbonized before burning. However, the gain disappears in more sophisticated stoves. In the developed world, the use of charcoal for fuel is rare, but for barbequing. Much of the “charcoal” which can be bought for this purpose, is however often not lump charcoal, but briquetted charcoal powder.

Soil amendment

Fine charcoal as soil amendment, or biochar, is an old practice, which still is in use. A famous example of this in the Amazon Basin, is the ‘terra preta’, which is Portuguese for black soil. Counterintuitively, the soil beneath the thin layer of humus in Amazon rainforest is highly weathered, nutrient poor, and not fit for farming. Amongst this reddish infertile soil are plots of land with fertile black soil up to 2 m deep. There is wide agreement that this soil is human made, either intentionally or unintentionally, and mostly of pre-Columbian origin, from 500 to 2,500 years old. It contains a large amount of charcoal and is fertile, rich in microbial life and resistant to the washing out of nutrients (Lehmann et al., 2007). Even though the char

itself is mostly carbon and highly inert, its porous structure has a high surface area provides a habitat for microbes and fungi. The self-sustaining nature of the terra preta has preserved it until today, and it is sought after both for farming, and even for sale as potting soil (Mann, 2002). The production, application and effects of biochar on soils is an active area of study, and is promoted both as an enricher of soils and long term carbon storage.

Metallurgy

Perhaps the most important role charcoal has played throughout human history is in metallurgy. To liquefy and cast most metals, intense heat is needed, and charcoal produces a higher temperature fire than does wood. In addition to being a source of heat, charcoal, more importantly, acts as a reducing agent separating the metal from the ore. The first emergence of extractive metallurgy is unknown, but evidence of copper smelting from present day Serbia suggests that it is a practice at least 7,000 years old (Radivojević et al., 2010). The technology is believed by some to have spread across Eurasia from here, but to have been independently discovered in for instance the Americas (Scattolin et al., 2010).

Fossil coal also has a long history of use in metallurgy, but in its raw form it tends to contain impurities such as sulphur, which lower the quality of the smelted metal. To purify the coal, is subjected to a destructive distillation similar to that used to convert wood to charcoal, but at higher temperatures. The process, called coking, removes impurities and produces coke, which is high in carbon content and allows the production of high quality iron without the use of charcoal. Evidence of the use of coke in metallurgy dates back to 400 AD in China (Wertime, 1962), but in Europe the technology was not known until around 1600 when the first methods of purifying coal were patented in Britain. Dwindling forests, and consequently rising wood fuel prices prompted the experimentation with coke fuelled iron production in Britain. In 1709 Abraham Darby was the first to produce iron of a quality comparable to charcoal-iron in a coke fuelled blast furnace. Throughout the 1700's Darby's technology was refined and spread in Britain, and eventually, to continental Europe. Besides being cheaper and increasingly available, coke also had the advantage of being mechanically stronger than charcoal, which was of importance, especially in large iron blast furnaces. The transition from charcoal to coke

facilitated the scaling and mass production of iron that played an important part in the industrial revolution. Today, coke dominates as reducing agent in smelting industries, but charcoal is still used, the Brazilian iron and steel industry being a notable example. Brazil is by far the largest producer of both wood charcoal and iron ore (Food and Agriculture Organization of the United Nations, 2015; Steel Statistical Yearbook 2016, 2016). Most of the iron ore is exported, but some is consumed in the domestic iron industry in which a third of the hot metal produced (about 10.2 million tons, 2007) is produced with charcoal in small blast furnaces (Augusto Horta Nogueira and Luiz, 2009; Machado et al., 2010).

Reintroducing charcoal in metallurgy

The blast furnace is a tall counter current furnace where the charge, i.e. the reducing agent, metal ore and often flux, is loaded from the top and oxygen-enriched air is injected at the bottom through what is called tuyeres. The reducing agents combust, and the resulting reducing environment liberates the iron from the iron ore and allows molten metal and slag to be collected at the bottom while flue gases are vented out at the top. Coke is essential to this process as a reducing and load bearing agent, and an energy source. Charcoal has properties making it an excellent reducing agent, potentially high fixed carbon content, low content of impurities like sulphur, nitrogen and mercury, low ash content in general and high surface area and reactivity (Antal and Grønli, 2003).

Larger blast furnaces require a mechanically stronger reducing agent, as the weight of the charge above is greater. It is important that the coke or charcoal are of a certain uniform size and retain it despite the weight of the charge above. If they shatter into finer particles, the gases may be blocked in some areas, reducing the gas permeability of the charge. Because of this the total replacement of coke by charcoal in large blast furnaces seems unlikely. A partial replacement is however possible. In some modern blast furnaces, an additional reducing agent is injected together with the air through the tuyeres to co-fire with the coke. The reductant supplied in this way can be gaseous, liquid or pulverized solids, like charcoal (Wei

et al., 2013). The amount of coke consumed in modern blast furnaces is around 350-400 kg ton⁻¹ hot metal, which could be halved to about 200 kg ton⁻¹ using auxiliary reductants like the ones mentioned (Suopajarvi et al., 2013).

The electric arc furnace is widely used in recycling of iron scrap and to produce metallurgical silicon. Although the load bearing requirement of the reducing agent is smaller in electric arc furnace than in the blast furnace, the mechanical stability of charcoal still poses a challenge. Finer charcoal particles, charcoal fines, easily become airborne and combust above the charge where they do not contribute to the process.

Wood structure and composition

Although a wide variety of feedstocks can be used to produce charcoal for various purposes, the charcoal used in metallurgy is preferably lump charcoal made from wood. Many of the properties of charcoal depend on its wood precursor, so careful feedstock selection is important for achieving a charcoal with the desired properties. Therefore, a basic understanding of wood structure and composition is useful.

Trees are seed bearing plants and can be divided into two major groups; gymnosperms and angiosperms. Belonging in the former category are conifers, or softwoods, and hardwoods belong in the latter. Softwoods are generally evergreen with needle-like leaves, like spruce and pine. Most hardwoods shed their blade-like leaves, seasonally in temperate conditions, while in tropical climates, the shedding can be more complicated and less regular. The terms hardwood and softwood can be misleading, as for instance, balsa wood is a very soft and light hardwood, and softwoods can be harder and denser than most hardwoods. About 30,000 species of hardwood are known, the vast majority of them tropical, and 520 softwoods. In Europe there are only 10 softwood and 51 hardwood species that exist naturally.

Structural components

The three main components of wood are cellulose (40-55%), hemicellulose (20-45%), and lignin (18-35%) (Thomas, 2000). The cellulose molecule is a linear homopolysaccharide with the chemical formula $(C_6H_{10}O_5)_n$ where n , the degree of polymerisation, can be more

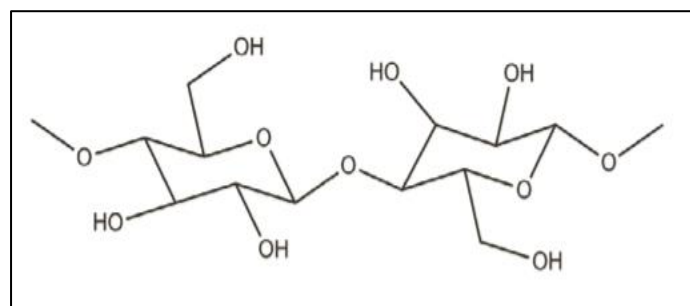


Figure 1: Cellulose represented by two linked glucose molecules (Kataki et al., 2015)

than 10,000 making it a long chain of glucose. These molecules form hydrogen bonds with one another and gather in bundles, or microfibrils, which have crystalline and amorphous regions. In the cell wall, these microfibrils are bound together by the hemicellulose and lignin.

The high tensile strength of wood can be traced back to the microfibrils which form cellulosic fibres, and the way in which these are aligned in the cell walls.

Hemicelluloses are matrix hetero-polysaccharides, which means that, as opposed to cellulose, they can be made up of several different monomers, and are branched molecules, rather than linear. They also have a lower degree of polymerisation than cellulose, normally around 200. The amount, structure and composition of hemicelluloses differ in softwood and hardwoods, and also depend on species and the part of the tree examined. The term holocellulose is a collective term encompassing both cellulose and hemicellulose.

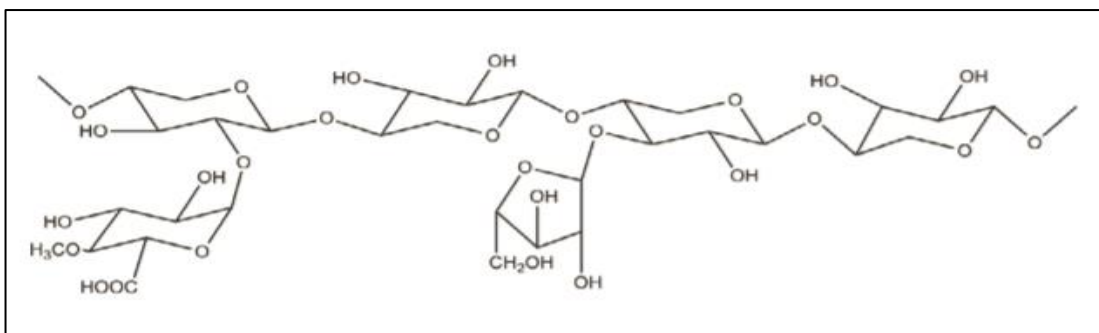


Figure 2: Hemicellulose, represented by different linked monomers (Kataki et al., 2015)

Lignin is a collective term for complex three-dimensional polymers of three different phenylpropane units with a degree of polymerization of 40-200. The structure of the lignins, and their proportions of the three phenylpropane are, again, different for softwoods and hardwoods. During wood cell formation, lignin enters late, and fills gaps in between the polysaccharide microfibrils, stiffening the cell wall, and increasing the

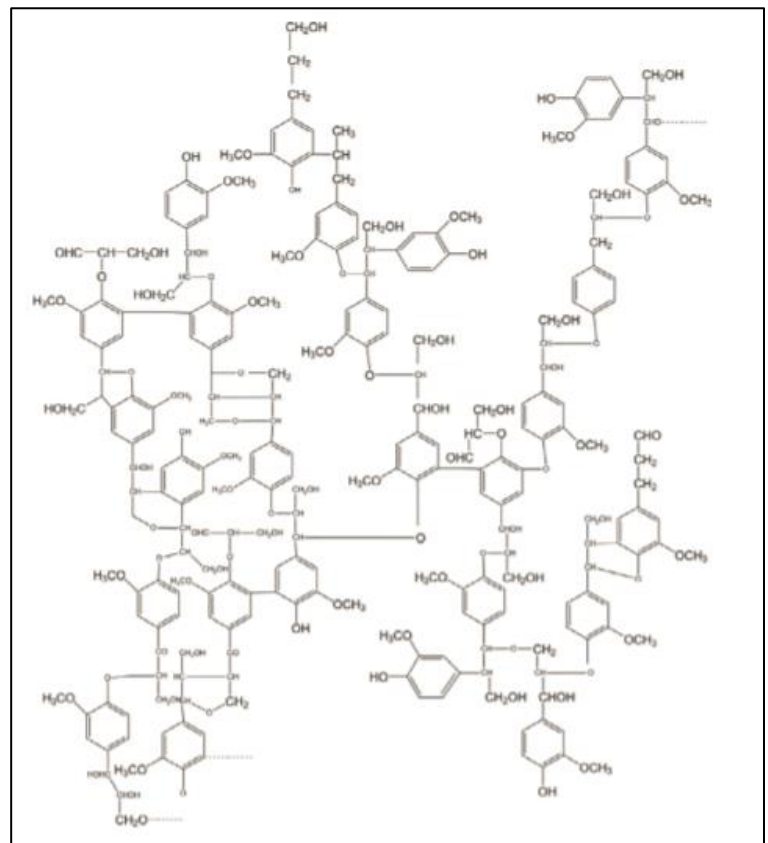


Figure 3: A sample lignin (Kataki et al., 2015)

compression strength of the wood (Barnett and Jeronimidis, 2003).

The lignin content is normally higher in softwoods than hardwoods at the expense of cellulose and hemicellulose. This is partly due to the different strategies of the two types of wood in coping with mechanical stress. Many softwoods generate what is known as compression wood, which is wood high in lignin that expands as it is formed. This kind of wood forms typically on the underside in leaning trees, and on the side facing downwind in areas with a predominant wind direction. In windy areas, compression wood may constitute 20-50% of the wood of a Scots pine (Thomas, 2000). Most hardwoods, on the other hand, apply a different strategy. They form tension wood high in cellulose, and comparatively low in lignin, on the opposite side of the tree from where compression wood would be formed. The tension wood contracts as it is formed, and thereby pulls, for instance, a leaning tree upright.

The effect of these strategies can be observed in the listed properties of 65 hardwood species and 47 softwood species common in the United States compiled in Wood Handbook – Wood as an Engineering Material (United States Department of Agriculture, 2010). The average compressive strength of the softwoods is about 90% of that of hardwoods, while the average density of the softwoods is only 77% of the density of the hardwoods. Additionally, if the compressive strength parallel to the grain is divided by the compressive strength perpendicular to the grain, the softwoods achieve an average ratio of 9.8 while it is 7.3 for the hardwoods.

Extractives

In addition to the structural components cellulose, hemicellulose and lignin, are the extractives. These are a vast number of different compounds soluble in polar or non-polar solvents. They include, fats, waxes, alkaloids, proteins, phenolics, simple sugars, pectins, mucilages, gums, resins, terpenes, starches, glycosides, saponins, and essential oils (Mohan et al., 2006). The content in wood is usually less than 10%, but can vary both in amount and composition in heartwood, sapwood, roots, branches, leaves and needles in the same tree (Sjöström, 1981). Although mostly non-structural and extracellular, they serve functions such

as intermediates in metabolism, energy reservoirs and protection against insect and microbial attacks.

Ash

The remaining inorganic non-combustible components of the wood after complete combustion is ash. The ash content of wood is seldom more than 1%, but can be substantially higher in bark and leaves. The ash contains a variety of elements often in the form of oxides. Misra et al., (1993) performed elemental analysis of the ash of pine, aspen, poplar and oak produced at 600°C that yielded calcium as the predominant element in all of them followed by either potassium or magnesium. An increase in temperature resulted in further weight loss, and a slight shift in the proportions of the elements. These findings of high calcium fit with the fact that many hardwoods and pines form calcium oxalate crystals from excess calcium in the water absorbed from the soil that reacts with oxalic acid in the cell sap.

Moisture content

The hydrogen bonds holding the cellulosic compounds together can also form bonds with water molecules, which makes them hygroscopic. When water is adsorbed in this way in the cell wall, it swells and its mechanical properties change. The bond formed with a water molecule, is a bond not formed with a neighbouring cellulosic fibre or lignin. A cell saturated with water is thus more malleable, and becomes more rigid as it dries. The fibre saturation point is defined as the moisture content at which the cell walls become saturated with water, and no free water exists. Its value varies among woods but has an average value of about 30% at 25°C, and decreases about 0.1% per 1°C rise in temperature (Grønli, 1996). This is taken advantage of by wood workers who will soak and heat up wood to be able to bend it, and then dry it in its new configuration, which it will then retain.

Moisture content exceeding the fibre saturation point is held as free water in the lumens or other cavities in the wood. Since the sapwood is responsible for water conduction, it tends to have a higher moisture content than the heartwood. In a newly harvested tree, the dry basis moisture content can range from 30-200% (Grønli, 1996).

Softwood structure

Softwood is mostly made up of elongated cells with a shape resembling a hexagonal prism aligned with the axis of the tree, called tracheids. They account for 90-94% of the wood volume, while the remaining 6-10% are radially aligned ray cells (Thomas, 2000). Not only are the

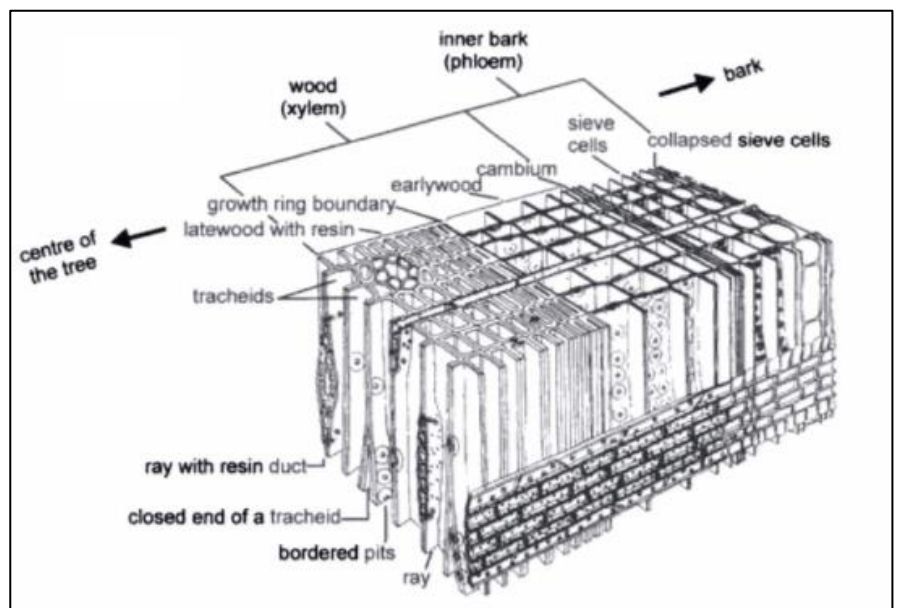


Figure 4: Softwood cellular structure (Schweingruber, 1966)

tracheids axially aligned in the wood, but most the cellulosic fibres, of which they are largely made up, are wrapped around the cell in a helical fashion making a non-zero angle with the transversal plane of the cell. This, along with its shape, gives the cell high tensile strength along its axis, and consequently the tree high tensile strength along the grain, about 40 times higher than perpendicular to the grain (Wainwright et al., 1982). The radial tensile strength is slightly higher than in the tangential direction due to the ray cells (Wainwright et al., 1982). Similarly, the compression resistance of softwood is about 10 times greater to forces applied parallel than perpendicular to the grain (United States Department of Agriculture, 2010). The tracheids are many times longer than they are wide, and perform the water conduction in softwoods. Since their ends are closed, the water conduction from one tracheid to another is done through openings in the cell wall, called pits. In temperate areas, the growth is strongest

in spring and early summer, and the wood formed in this period is called earlywood. The tracheids in this wood have thinner cell walls, larger lumen, and a higher number of pits to facilitate water conduction. The latewood, forming towards the end of the growing season, consists of sturdier tracheids with thicker walls. The difference in earlywood and latewood is discernible as growth rings in the cross section of a log.

The ray cells are strips of living tissue running from the centre of the tree, the pith, to the phloem just inside the bark, present in both softwoods and hardwoods. They perform radial water conduction, and storage of resources, like starches, fats and nutrients when produced in excess, or withdrawn from the leaves before leaf shedding (Thomas, 2000).

Hardwood structure

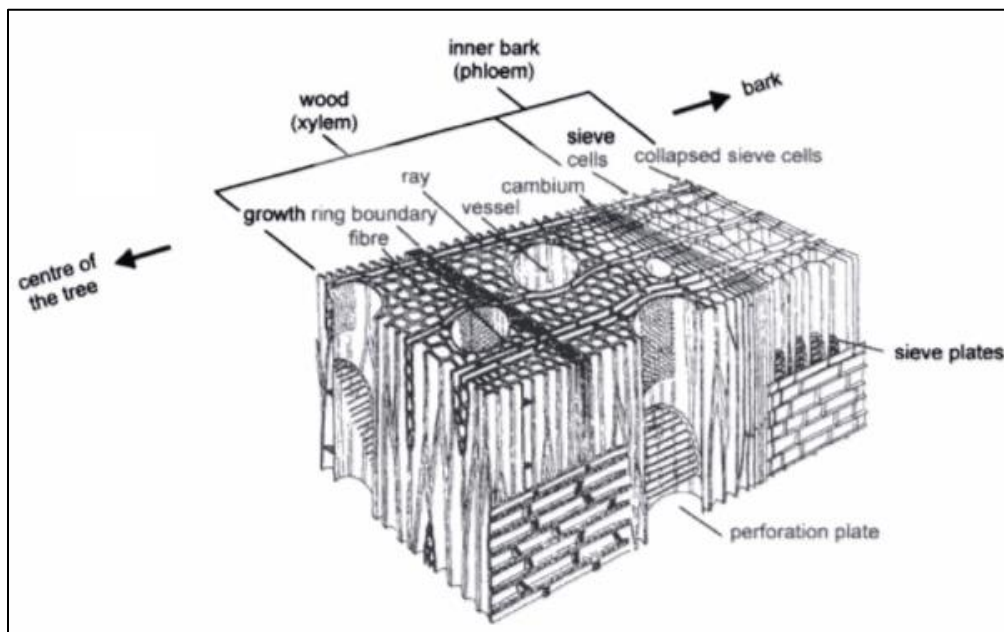


Figure 5: Hardwood structure (Schweingruber, 1966)

The structure of hardwoods is more complex than that of softwoods, as it consists of a wider variety of cells. The three main types of cells and their average portion of the wood volume are: the conducting vessels (30%) the supporting tissue (50%) and the ray cells (20%) (Thomas,

2000). The vessels are made up of short and up to 0.5 mm wide vessel elements. These are connected end to end to form a tube which can be a mere centimetre long, or in some cases, run the entire length of the tree. They are efficient water conductors which is needed for instance during leafing, and rapid growth of many hardwoods. Where they are in contact with other vessels or rays, they have pits similar to those in softwood tracheids. The supporting tissue includes a hybrid of the supporting and conducting tissue labelled fibre tracheids similar to the tracheids found in softwood. The more common supporting tissue are the long, slim, thick walled libriform cells, which are bound together in a matrix supporting the vessels. Hardwood ray cells are similar to, and serve the same purpose as those in softwood, but are generally more complex, thicker and in some species there are parts of the ray circuit running axially.

The large vessels are wide enough to be seen with the naked eye in a cross section of the wood, and they are commonly called pores. Some hardwood species form many large diameter vessels at the beginning of the growing season, and later only smaller ones. This is common in temperate areas with a limited growing season. These are known as ring-porous as there will be a thin ring with wide pores in each growth ring. The diffuse-porous woods have their pores more evenly spread across the radius of the growth ring, or there is an absence of a growth ring altogether in some tropical species (Thomas, 2000). This difference is of importance to wood workers as the ring-porous woods come with a structural weakness where the large vessels are concentrated.

Sapwood and heartwood

Sapwood is the living part of the tree active in cell growth beneath the bark, conduction and other physiological processes. In young trees this is the entire, or a large part of the stem. As the tree grows, the innermost cells die and form heartwood which is physiologically dead tissue. The heartwood portion grows to comprise most of the stem in older trees. Often, the transition between sapwood and heartwood can be seen as an abrupt change in colour in the cross section of a tree, but not for all species. Partly responsible for the change in colour is the formation of various extractives as the cells die to form heartwood. In some species, this

makes the heartwood sturdier, denser, and more resistant to rot. In softwoods, heartwood formation is also associated with the closing of the pits connecting the cells. This, in addition to the extractives clogging the previously water conducting pathways, can make heartwood dry slower than sapwood (Bamber, 1961).

Pyrolysis of wood

Pyrolysis is the thermal decomposition of organic matter in the absence of oxygen. The resulting substances take gaseous, liquid and solid forms. Four of the major types of pyrolysis are summarized in table 1.

Table 1: Pyrolysis types (Ronsse et al., 2015)

	Pyrolysis type			
	Fast pyolysis	Carbonization	Gasification	Torrefaction
Temperature	~500°C	>400°C	600-1800°C	<300°C
Heating rate	Fast, up to 1000°C min ⁻¹	<80°C min ⁻¹	-	-
Residence time	Few seconds	Hours or days	-	<2h
Pressure	Atmospheric (and vacuum)	Atmospheric, or up to 1MPa	Atmospheric, or up to 8MPa	Atmospheric
Medium	Oxygen-free	Oxygen-free or oxygen-limited	Oxygen-limited (air or steam/oxygen)	Oxygen-free
Liquid yield	75%	30%	5%	5%
Non-condensable gas yield	13%	35%	85%	15%
Char yield	12%	35%	10%	80%

In addition to the parameters listed in the table above, the choice of feedstock is also important in determining the qualities and relative proportions of the products of pyrolysis. The type of pyrolysis considered in this work, is carbonization and torrefaction using wood or wood-like biomass as feedstock. The three major wood components decompose at different rates at different temperatures. Typical mass loss and rate of mass loss is given in figure 6 a and b respectively for cellulose, hemicellulose (represented by xylan), and lignin.

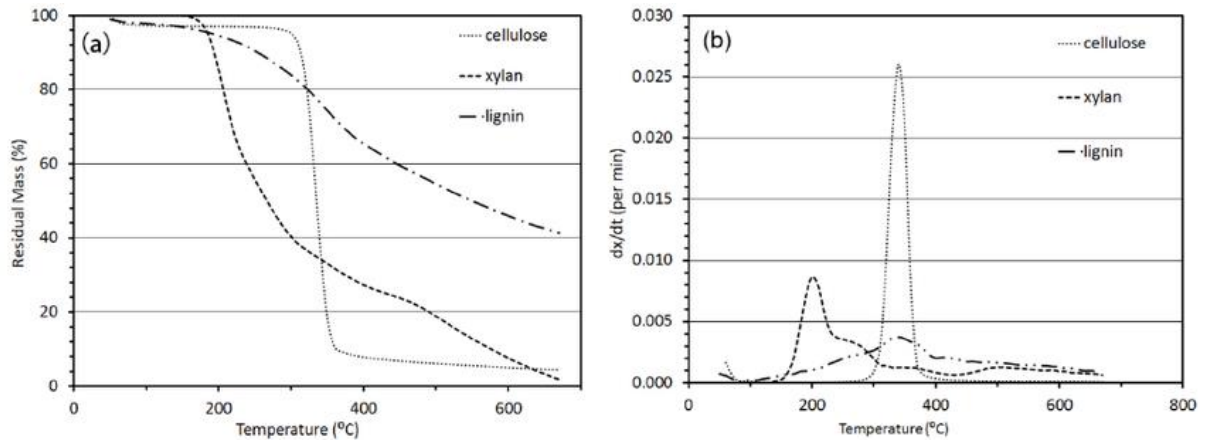


Figure 6: Typical mass loss (a) and rate of mass loss (b) as a function of temperature for cellulose, lignin and hemicellulose (represented by xylan). (Jin et al., 2013)

The free water, if any is present, is the first to evaporate followed by the bound, or hygroscopic, water. The cellulose and hemicellulose begin their decomposition in much the same way with a decrease in the degree of polymerization, which has been found, in the case of cellulose, to begin at temperatures as low as 70°C (Gaur and Reed, 1998). Torrefaction is mild pyrolysis in the temperature range 200-300°C. The weight loss occurring in the torrefaction temperature range is mainly due to thorough drying, evaporation of the more thermally reactive volatile compounds, and thermal degradation of hemicellulose and some lignin. Dry basis mass density decreases while heating value [kJ/kg] increases. The torrefied wood becomes more brittle, resistant to biological decay and less hygroscopic (Antal and Mok, 1990). From about 170 to 270°C the wood produces CO and CO₂ off-gases in addition to gases which can be condensed and refined to pyrolysis oil (Emrich, 1985). As the temperature rises above that of the torrefaction zone, weight loss resulting from the degradation of cellulose commences. Due to its homogeneity, its rate of weight loss peaks sharply, as depicted in figure 6 b, typically somewhere between 320 and 380°C (Gaur and Reed, 1995). Because often more than half of the wood mass is cellulose, this coincides with the most rapid mass loss in the wood. The lignin decomposes more gradually and over a wider temperature range than the cellulosic compounds. Lignin preferentially forms char when it decomposes, and due to the differences in lignin compositions between species, much can be known about the feedstock from examining the products from its pyrolysis (Gaur and Reed, 1998). In a retort operated in batch mode, external heat is needed at first, either from an external source or from partial combustion of the feedstock, but at around 270-280°C exothermic reactions start, and the temperature climbs to 400-450°C and stabilizes (Emrich, 1985). To increase the

temperature further, external heat is needed. After the onset of the exothermic phase, the production of CO and CO₂ ceases, but more condensable gases are produced.

Although some woods, like spruce, can swell during pyrolysis, most woods shrink (Antal and Grønli, 2003). E. A. McGinnes et al., (1971) performed slow pyrolysis on pieces of oak with HTT of 277-398 °C observing structural and anatomical changes in the wood. The dimensional shrinkages, as they relate to the growth rings, were from the most to the least: tangential, radial and axial. This uneven shrinkage can result in radial cracks in the charcoal, particularly at higher heating rates.

The mass loss of the wood is generally more severe than the shrinkage, resulting in a lower density in the charcoal compared to the wood feedstock. The density decreases with increasing temperature as volatile matter evaporates up to a HTT of around 600°C. A further increase in temperature has been found to slightly increase the density of the charcoal for several wood species (Blankenhorn et al., 1978; Kumar et al., 1999). This has been attributed to the cracking and deposition of pyrolytic carbon in the pores of the charcoal. As temperatures approach 1000°C and beyond, the char formed takes on a more ordered, layered honeycomb structure, resembling that of graphite.

Primary and secondary reactions

Charcoal is often considered to be the product of two separate classes of reactions: primary and secondary reactions. Primary reactions are the solid phase generation of charcoal, while secondary reactions are a result of the decomposition of volatilized tarry organic vapours producing char and non-condensable gases (Antal and Grønli, 2003). Non-condensable in this context means not easily condensable by cooling, which applies for instance to CO, CO₂, and CH₄. Promoting the occurrence of secondary reactions thus favours the generation of char at the expense of condensable gases. Secondary reactions are highly exothermic compared to the more endothermic primary reactions (Ronsse et al., 2015).

Proximate analysis

A common way to analyse and determine the quality of charcoal is through proximate analysis. The charcoal is then regarded as consisting of four components; moisture, volatile matter, fixed carbon and ash. ASTM standard D 1762 – 84 is a commonly applied standard to determine the proportions of these components (Standard Test Method for Chemical Analysis of Wood Charcoal, 2013). The procedure is essentially as follows. The samples are ground to a powder, one gram of which is placed in a ceramic crucible. The moisture content of the sample is found from the weight loss in a drying oven maintained at $105\pm 1^\circ\text{C}$ for 2 hours. Then follows a 10-minute stay in a 950°C muffle furnace with a lid on the crucible. The weight loss in this period is defined to be volatile matter content. Finally, the crucibles are put into a 750°C muffle furnace without a lid for 6 hours to allow complete combustion. The mass now left in the crucible is the ash content, and the fixed carbon content is defined to be the weight of the dried sample which is neither volatile matter nor ash.

Maximum fixed carbon yield

Metallurgical charcoal should have a high fixed carbon content, around 85-90% according to (Foley, 1986), as it is the carbon which removes the oxygen from the metal ore in the furnace. For the trading of metallurgical charcoal, the fixed carbon content therefore commonly determines the price of the charcoal (Antal and Grønli, 2003). The charcoal manufacturer is therefore interested in the charcoal yield or fixed carbon yield compared with the dry weight of the wood feedstock, insofar as wood price and/or production capacity are limiting factors. The fixed carbon yield can be defined as

$$\gamma_{fC} = (m_{char}/m_{bio}) \times (\%fC/100 - \% feed ash)$$

where m_{char} is the dry mass of the charcoal, m_{bio} is the dry basis mass of the feedstock, %fC is the fixed carbon content of the charcoal found by proximate analysis, and % feed ash is the dry basis ash content of the feedstock. This is thus a measure of the fraction of the feedstock

converted to fixed carbon, disregarding the ash. When the elemental analysis of the feedstock is known i.e. the mass fractions of carbon oxygen and hydrogen, these can be input in a thermochemical equilibrium calculating software along with two thermodynamic constraints, like final temperature and pressure. The software then outputs the mass fractions of solid carbon and non-condensable gases at thermochemical equilibrium. This fixed carbon yield can be regarded as the upper theoretical limit that can be achieved through a thermal process, and can thus serve as a benchmark with which experimental fixed carbon yield can be compared to evaluate the efficiency of the pyrolysis process. In this idealised simulation, all condensable gases are allowed to reach equilibrium and be carbonized. In practice, some of these gases are often vented out of the heated region before reaching equilibrium, which constitutes a loss of carbon which is reflected in a lower char- and fixed carbon yield. Biomass samples in pyrolysis chambers with no gas venting and elevated pressures approach, and can effectively reach this theoretical maximum char yield (Antal Jr et al., 2000). Traditional kilns commonly do not achieve an efficiency exceeding 40%, partly due to the loss of carbon in organic compounds leaving the heated zone with other gases, and the allowance of some combustion in the kiln (Antal and Grønli, 2003).

Feedstock composition and char yield

Lignin is known to preferentially form char during pyrolysis (Antal and Grønli, 2003; Antal Jr et al., 2000). At lower heating rates, a char yield of 50% from isolated lignin has been achieved (Gaur and Reed, 1998). This is partly because lignin has a higher carbon content (60-63%) than for instance cellulose (44.4%) (Mackay and Roberts, 1982). This gives wood high in lignin more carbon available to be fixed, but the fixed carbon yield of lignin rich biomass is often higher than what would be expected from the increased carbon content alone. Mackay and Roberts, (1982) pyrolyzed various biomasses with lignin contents ranging from 0 to 70.3% and the biomasses with the higher lignin content generally formed more char per mass of available carbon in the feedstock. Lignin has a less straight-forward thermal decomposition pathway than its cellulosic counterparts, and decomposes across a wider temperature range. This

would seem to favour softwoods in terms of fixed carbon yield, as their lignin content is generally higher than that of hardwoods.

The hemicelluloses have a carbon content comparable to the cellulose. They do however largely lack the crystalline structure found in cellulose microfibrils that is known to increase the char yield (Mackay and Roberts, 1982). The hemicelluloses are also more reactive than the cellulose and has its peak rate of mass loss at a lower temperature. Cellulose and hemicellulose both produce more volatiles than lignin. The condensable fraction of these is larger for cellulose than for hemicellulose (Kataki et al., 2015). Modelling the pyrolysis of wood by simply summing of the behaviour of the isolated lignin, hemicellulose and cellulose, like in figure 6, can offer a decent predictions of yields from pyrolysis. However, there are complex interactions between all three when wood is pyrolyzed, which can influence gas, liquid and char yield (Kan et al., 2016).

The content and composition of ash in the wood can also influence the char yield. The contamination of cellulose with various inorganic flame retardants is known to decrease the temperature at which weight loss begins, and to increase the char yield upon pyrolysis (George and Susott, 1971; Tang and Neill, 1964). These inorganic compounds are believed to have a catalytic effect on char forming, which increases with their content up to a saturation point of 2-15% (Mackay and Roberts, 1982). Not all inorganics have this effect on the pyrolysis process, however. Mutch and Philpot, (1970) suggest that for two common grass species, the silica fraction of the ash can be disregarded as an influencer of pyrolysis processes. Although more abundant in grasses than wood, silica beads can be found in some tropical wood species (Thomas, 2000). Yet other inorganic substances can have the effect of reducing char yield. The increased char yield found upon deashing groundnut shell, rice husk and coir pith has been attributed to high potassium contents in the ash (Raveendran et al., 1995).

Temperature

The highest treatment temperature is a very influential factor in determining the fixed carbon content of charcoal. Increasing the temperature causes volatile matter to vaporize or solidify, approaching a state of only fixed carbon and ash, which is at most 950°C by the definition of fixed carbon content. Figure 7 shows the char yield (residue yield), fixed carbon content and fixed carbon yield of beech as a function of carbonization temperature, with heating rates 2 °C min⁻¹ (solid line)

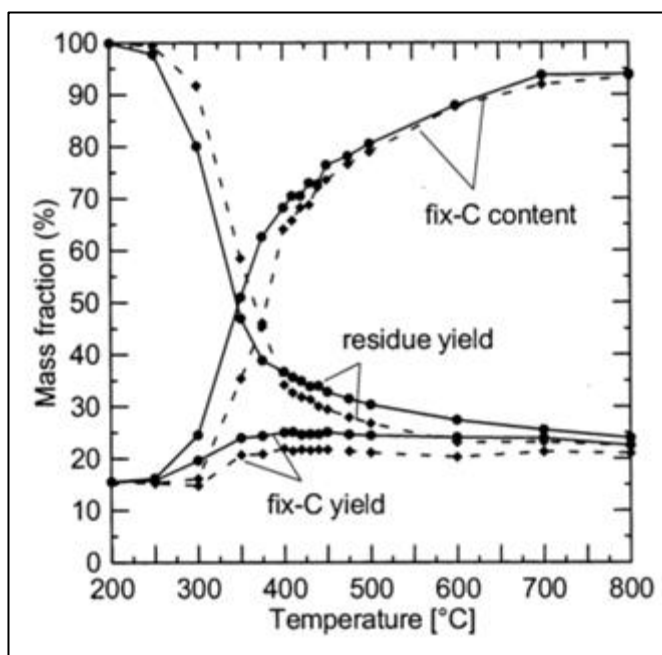


Figure 7: Carbonization of beech (Schenkel, 1999)

and 10°C min⁻¹ (dotted line). It displays the char yield initially dropping fast in the range of cellulose decomposition, and stabilizing as the fixed carbon content tends to (100 – ash content) [%]. In internal heating pyrolysis installations where the temperature is regulated by the partial combustion and other exo- and endothermic reactions in the feedstock, it plateaus at around 450-500°C (723-773K), which generally leaves a significant amount of volatile matter (Emrich, 1985).

Not only is the peak temperature an influential factor in determining the yields from pyrolysis, but also the rate at which this temperature is approached, which is referred to as the heating rate. A practically instant temperature increase from room temperature to >500°C can cause small wood particles to almost completely evaporate, leaving virtually no char (Antal and Mok, 1990). Secondary reactions predominate if vapour residence times, the time spent by the tarry vapours in the heated zone close to the char, of >1s are allowed (Ronsse et al., 2015). This can account for some of the decreased char yield at high heating rates because the generation of volatiles is faster. Slowing the heating rate normally increases the char yield to a point after which a further decrease has little or no effect. This point may be in the order of 100°C min⁻¹ or in the single digits depending on the installation and feedstock (Antal and

Grønli, 2003; Antal and Mok, 1990). An increased heating rate is also associated with producing a higher number of cracks in the charcoal, and decreasing its mechanical strength (Antal and Grønli, 2003; Kumar et al., 1999; Noumi et al., 2014).

Particle size, pressure and flow rate

As larger particles carbonize, and the heating rate is not very slow, what is known as a pyrolysis front is formed. This is the boundary between the outer carbonized layer and the inner un-carbonized core. The pyrolysis front moves inwards, eventually carbonizing the entire particle. As volatiles in the core evaporate, they have to pass through the carbonized layer where they can undergo secondary reactions, forming char. Above 550°C, particle size play less of a role in char formation due different volatiles evolving at these temperatures (Antal and Grønli, 2003).

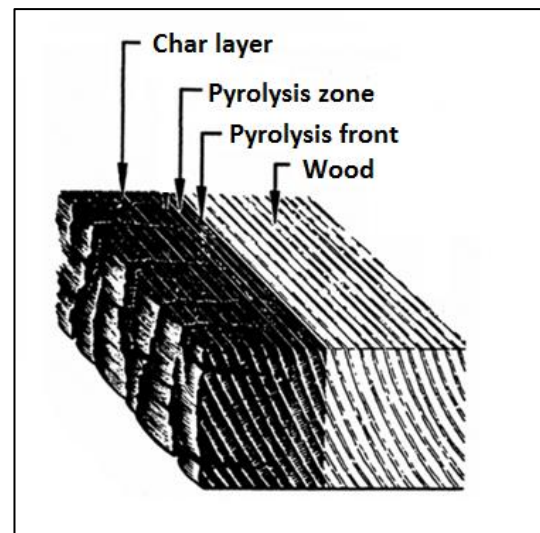


Figure 8: Pyrolysis front (United States Department of Agriculture, 2010)

If the tarry vapours are quickly vented out or carried out by some carrier gas, the vapour residence time decreases, and there can be a loss of potentially char forming carbon, decreasing the char yield. Similarly, at elevated pressures, the proximity of the particles in the vapours increases, and secondary char forming is enhanced.

Measurement of density and porosity

The density of a substance seems like a straight forward quantity to obtain, dividing its mass by the volume it occupies. Complications arise when dealing with granular substances, like powder or pebbles, and porous substances, like charcoal, complicate things further.

A very crude way to measure bulk density of charcoal is filling a container of known volume with charcoal of known weight. This will give a density varying with the granulometry, i.e. particle size distribution of the charcoal.

There exists a standard for measuring the apparent and true gravities of coke (Standard Test Method for Apparent and True Specific Gravity and Porosity of Lump Coke, 2012) which has been adapted and applied to charcoal by some authors (de Assis, 2007; de Oliveira et al., 1982c). For apparent gravity, particles of a representative size are immersed in water for 15 minutes, and the specific gravity is calculated as

$$\text{Apparent specific gravity} = \frac{A}{(B+(C-A))}$$

where A is the mass of the dry coke, B is the mass of water displaced by wet coke, and C is the mass of the wet coke.

Measuring the true gravity, the coke is ground to a size <75µm and immersed in water, which is then boiled for one hour.

$$\text{True specific gravity} = \frac{D}{(D-(E-F))}$$

where D is mass of dry coke, E is the mass of dry coke, bottle and water required to fill it, and F is the mass of the bottle and water required to fill it. The porosity can then be calculated as

$$\text{Porosity} = 100 - 100x \frac{\text{Apparent specific gravity}}{\text{True specific gravity}}$$

The porosity of charcoal largely stems from its retention of the cellular structure of the wood feedstock. With increasing carbonization temperature, the porosity of charcoal increases as water and other volatiles, stored in the lumens, vessels or other cavities in the wood, evaporate. Once a certain temperature is reached, however, a further rise in temperature can cause a decrease in porosity as secondary char is deposited in the pores. For cherry wood this temperature has been found to be near 700°C (Blankenhorn et al., 1978).

A simpler way to measure the apparent density, or particle density is coating an individual particle of known mass in a water repellent, and submerging it in water to determine its

volume. This will give a similar, but slightly lower, value than the one obtained in the equation for apparent density above, because it disregards small cracks and large pores on the surface of the particle. Since the reference medium in calculating apparent and true specific gravity is water, the values obtained can be given units of $[g\ cm^{-3}]$ by measuring, or looking up tabulated values for, water density at the measured water temperature.

Mechanical strength of charcoal

The mechanical strength of charcoal is, as mentioned, one of the main obstacles to its replacing fossil reductants in metallurgy. Through handling and transport of the charcoal from production to consumption, it is subjected to various stresses which produce charcoal fines in the size range of millimetres and smaller. The amount of these, depending on the feedstock and pyrolysis conditions, is around 10-25% of the total volume straight out of the kiln, and during transport and handling another 10-20% can be produced (Kristoferson and Bokalders, 1987). Oliveira (1982) claims that the total amount is about 25%, from the production of the charcoal, transport, handling and sieving, prior to consumption. The fines are generally unwanted in the charge in both blast furnaces, electric arc furnaces and others as they decrease gas permeability in the charge, and may be carried away by the flue gases. Tightly packed smaller charcoal particles are also more likely to spontaneously combust than larger lump charcoal during transport and storage. In 1985 it was claimed, that charcoal was the most expensive material going into blast furnaces (FAO Forestry Department, 1985). Steps taken to reduce the generation of fines thus appear worthwhile. A way to simulate the handling and transportation of charcoal is to perform a friability test in a tumbler drum. In the tumbler drum, the charcoal is subjected to shear and impact stresses, and the friability of the charcoal is quantified as a reduction in particle size after treatment. The HGI is measured to estimate the energy requirements in grinding a substance, but it is quantified, like tumbler drum friability, by measuring a reduction in particle size. These two tests, and the performance of various pyrolyzed biomass in them, are discussed below. First the compressive strength of charcoal is discussed. This is a different, but related property of the substance in that compressive stress is prevalent in a HGI mill, and can also contribute to the generation of fines.

Compressive strength

The compressive strength, compression resistance or crushing strength refer to the ability of charcoal to resist compressive force without significant fracturing. The measurement of this property in single monolithic charcoal particles is commonly done by placing lump of charcoal between two parallel surfaces. The charcoal particle should have reasonably flat sides facing each surface. One of the surfaces is then slowly made to move towards the other while the resistance it meets in contact with the particle is measured as a force. When fracturing of the charcoal occurs, the force applied at that moment represents the compressive resistance. This corresponds to the peak of a stress-strain graph (figure 9).

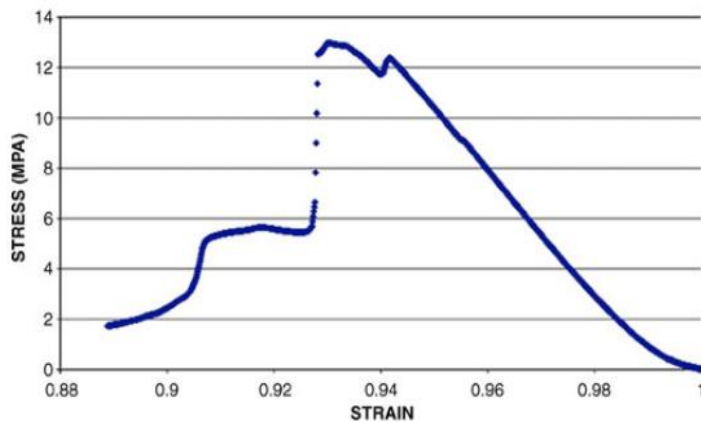


Figure 9: *Salvadora oleoides*, treated at 200°C and compressed parallel to fibres (Lancelotti et al., 2010)

The force applied is then divided with the cross-sectional area yielding pressure (Pa) or mass per area (kg cm^{-2}).

Kumar et al., (1999) performed compressive strength tests on charcoal made from *Eucalyptus* sp. and *Acacia* sp. carbonized at temperatures ranging from 270-1200°C. The compressive strength vs carbonization temperature they measured is given in figure 10.

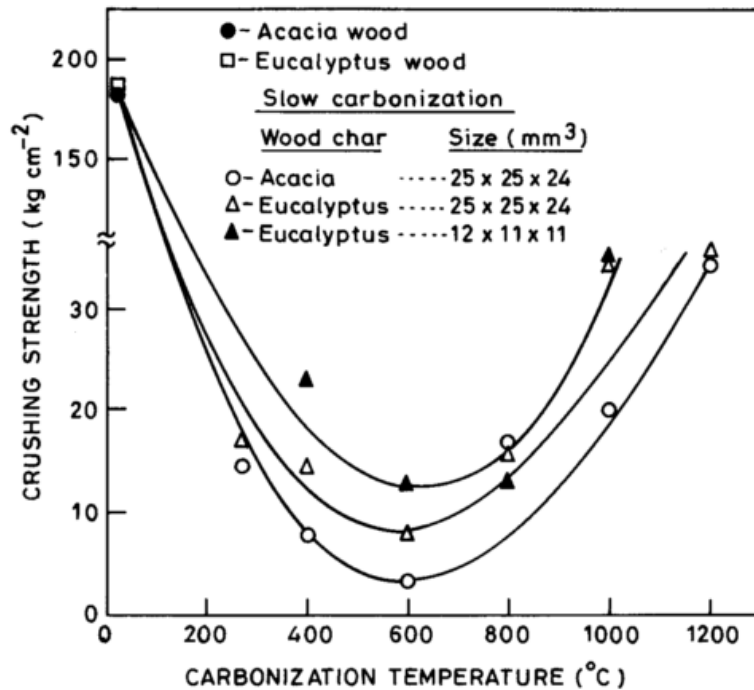


Figure 10: Compressive strength (crushing strength)(Kumar et al., 1999)

The compressive strength decreases with temperature to reach a minimum at around 600°C. A further increase in temperature causes the charcoal to regain some of its compressive strength. A similar increase in compressive strength as the temperature rises from 600°C has been found by others (de Assis, 2016; de Oliveira et al., 1982c; Vieira, 2009). Kumar observed dimensional shrinkage throughout the temperature range, but the apparent density followed a trend like that of the compressive strength with a minimum value at around 600°C. A minimum apparent density for charcoal around 500-600°C has also been found by others for several wood species (Blankenhorn et al., 1978; Slocum et al., 1978). The increase in density was attributed by Kumar et al. to the condensation of carbon microcrystallites and pyrolytic carbon deposition in the pores of the charcoal. The crushing strength depicted in figure 10 was achieved using a heating rate of 5°C min⁻¹. Kumar found that increasing the heating rate to 30°C min⁻¹ significantly lowered the compressive strength. The inverse relationship between heating rate and compressive strength in charcoal has also been found by others (Monsen et al., 1997; Noumi et al., 2016).

Because the anisotropic nature of wood is preserved through pyrolysis, a higher compressive strength is measured if force is applied parallel rather than perpendicular to the grain. The

ratio has been found to be around 3-4 for pine and various softwoods (Lancelotti et al., 2010; Monsen et al., 1997). De Assis found the ratio to be 7-9 for Eucalyptus carbonized at 500°C and 900°C. She also found a slightly higher compressive strength when compression was done radially compared to tangentially (de Assis, 2016). The location of sample in the tree can also influence the compressive strength of charcoal. Vieira found that charcoal made from wood close to the bark was significantly more resistant to compression along the fibres than charcoal from wood closer to the centre (Vieira, 2009). The effect persisted from carbonization temperatures of 350°C to 900°C.

Charcoal is known to have a far inferior compressive resistance to fossil coke, and this is commonly stated as one of the primary obstacles to replacing fossil coke with charcoal in large blast furnaces. Typical compressive strengths for charcoal and coke are given in table 2.

Table 2: Charcoal and coke requirements (Rousset et al., 2011)

Parameters	Steel quality charcoal		Steel quality coke	
	Charcoal	charcoal	coke	Coke
Fixed carbon [%]	65–75	74–77	88	88–92
Volatile matter [%]	25–35	25–22	1	7.8–11
Ash [%]	2–5	1–1.5	10–12	0.1–0.5
Compressive strength [kg cm ⁻²]	10–80	50–100	130–160	–

Since the position of the charcoal in the charge in the furnace is random, the compressive strength to be considered should be the lower one, i.e. the one where the load is applied perpendicular to the fibres. Some achieved values for compressive strength perpendicular to fibres for charcoal are listed in table 3 for comparison with table 2.

Table 3: Compressive strength of some charcoals

Source	Biomass	Compressive strength		Carbonization temperature
		[kg cm ⁻²]	[MPa]	[°C]
Emmerich and Luengo, (1996)	Babassu nut	1019	100	1000
Lancelotti et al., (2010)	<i>Senna auriculata</i>	61	6	400
Oliveira, (1982)	<i>Eucalyptus grandis</i>	51	5.03	900
Kumar et al., (1999)	<i>Eucalyptus</i> sp.	36	3.53	1200
	<i>Acacia</i> sp.	35	3.43	1200
de Assis, (2016)	<i>Eucalyptus</i> sp.	29	2.8	900

The obvious outlier in table 3 is the babassou nut. It is a fist sized nut that when carbonized unbroken, can achieve compressive strengths far surpassing the requirements for metallurgical coke. Even at carbonization temperatures of 400 and 600°C Emmerich measured compressive strength of about 25 [MPa], or 250 [kg cm⁻²]. With the exception of the *Senna auriculata* charcoal, the carbonization temperatures in table 3 are so high that practically no volatile matter would be present.

A way to achieve a bio based reductant with acceptable compressive strength is briquetting charcoal fines. Quicker et al., (2011) managed to produce a bio-coke-briquette with a crushing strength twice that of a reference coke, using molasses (12% wtdb) and clay cement containing iron and quartz particles (12% wtdb) as binders. Although a high durability can be achieved, briquetting can be an involved process, and the composition and amount of the binders required can make it costly, and give the product unwanted properties such as an elevated ash content.

Data analysis

Data gathered from the literature is now presented and analysed. The tumbler test section contains data from seven sources with data from tumbler drum friability tests on charcoal from various species. The first to be analysed out of these is from a book consisting of a collection of papers (de Oliveira et al., 1982c). It contains analyses of a wide range of charcoal properties, friability being one of them, and also the tumbler test itself. The data is discussed and subjected to additional analysis. Next are the six more limited sources also presenting data on charcoal friability (de Assis, 2007; Coutinho and Ferraz, 1988; Gomes da Silva et al., 2007; Lana, 2012; Noumi et al., 2014; da Silva et al., 2014). The number of charcoal properties and experimental settings is smaller for these, but an attempt is made to make comparisons where possible. The second section is the analysis of data from three studies which have measured the grindability, and several other properties, of torrefied biomass. Since these sources presents grindability in terms of the well-defined HGI, they are analysed together.

Friability tumbler tests

The first study in the book “Carvão vegetal: destilação, carvoejamento, propriedades, controle de qualidade” consists of preliminary tumbler drum test obtaining optimal testing parameters for further testing (de Oliveira et al., 1982b). Some of the results are summarized in the following. The standard for tumbler test of charcoal NBR 8740 (ABNT, 1985) recommends rotation of the drum at 30 RPM, a speed which Oliveira found to produce more fines < 13mm compared to a slightly increased or decreased speed. Keeping an RPM of 35, the number of rotations was found to increase the number of fines <13mm roughly linearly up to about 500, after which the generation of fines tapered off slightly. An increase in the mass of charcoal loaded into the drum, from 15kg to 20kg and 25kg was found to decrease the amount of fines generated, and was attributed to the cushioning effect of the increased volume of charcoal. Reducing the particle size range, keeping other parameters fixed,

decreased the generation of fines. The apparent increased strength of smaller particles was attributed to the propensity of larger particles to develop internal cracks during carbonization.

Next, with testing parameters obtained from the preliminary studies, 27 samples of charcoal from *Eucalyptus grandis* were tested in a tumbler drum. Carbonization temperatures were 300, 500 or 700°C, slow heating rate (0.5°C min⁻¹), and a soaking time so the area under the temperature vs time graphs for the different temperature treatments were the same. This amounted to approximate residence times at peak temperature of 40 h, 19 h and 7 h for carbonization temperatures 300°C, 500°C and 700°C, respectively. The tumbler tests were carried out with a drum of diameter 30 cm and length 25 cm in which 500g of charcoal was spun at 35.5 RPM for 500 rotations.

As independent variables water content of feedstock, age of wood feedstock and highest treatment temperature were chosen. To be able to assess the independent effects of the three independent variables, tree age, moisture content, the samples were chosen so that for each of the three levels of the independent variables, the average value of the other two independent variables were the same or similar. These levels have been colour coded in table 4 to illustrate this. The friability was taken as the percentage of initial mass <13 mm after tumbling. The obtained data is presented in table 4.

Table 4: Wood and charcoal properties (de Oliveira et al., 1982a).

Age [yrs]	Water [%wb]	Temp [°C]	FC [%db]	Ash [%db]	VM [%db]	GY [%db]	D [g cm ⁻³]	TD [g cm ⁻³]	P	Fri [% 13 mm]
6	15.43	300	71.09	1.5	27.41	38.6	0.3	1.31	77.1	10.4
6	16.72	500	84.86	1.96	13.18	34.14	0.31	1.43	78.32	10.7
6	14.83	700	91.29	2.73	5.98	28.81	0.29	1.61	81.99	10.1
6	24	300	68.39	1.76	29.85	41.55	0.29	1.34	78.36	9.4
6	25.8	500	82.86	1.43	15.71	32.5	0.33	1.35	75.56	12.5
6	24.5	700	91.49	2.84	5.67	30.07	0.35	1.65	78.79	10.7
6	36.7	300	67.79	0.76	31.45	37.81	0.31	1.35	77.04	14.7
6	46.22	500	88.4	0.79	10.81	29.97	0.35	1.35	74.07	15.7
6	45.59	700	92.75	1.21	6.04	29.66	0.39	1.68	76.79	13
8	15.93	300	68.67	0.81	30.52	41.77	0.38	1.36	72.06	12.3
8	15.17	500	86.21	1.1	12.69	33.12	0.33	1.43	76.92	12.9
8	16.77	700	93.61	1.17	5.22	30.07	0.46	1.7	72.94	10.7
8	25.7	300	70.82	0.94	28.24	38.2	0.4	1.38	71.01	13.9
8	22.4	500	85.86	3.18	10.96	33.04	0.38	1.34	71.64	17.1
8	25.12	700	91.59	1.64	6.77	31.6	0.39	1.74	77.59	17.5
8	36.1	300	65.32	0.72	33.96	43.24	0.51	1.41	63.83	19.7
8	36.1	500	85.38	0.98	13.64	30.66	0.39	1.43	72.73	19.8
8	36.1	700	90.58	1.38	8.04	30.21	0.46	1.62	71.6	19.5
10	16.92	300	70.81	0.58	28.61	37.87	0.37	1.39	73.38	11.8
10	15.75	500	85.89	0.73	13.38	33.84	0.38	1.39	72.66	12.9
10	15.87	700	93.17	0.94	5.89	29.04	0.42	1.69	75.15	8.6
10	27.25	300	67.34	0.55	32.11	43.63	0.39	1.41	72.34	14.3
10	25	500	86.86	0.64	12.5	31.64	0.37	1.4	73.57	14.5
10	23.5	700	92.99	0.96	6.95	32.64	0.37	1.71	78.36	12.1
10	35.6	300	61.92	0.92	37.16	46.31	0.52	1.29	59.69	12.3
10	35.76	500	85.06	1.08	13.86	36.57	0.35	1.44	75.69	15.1
10	33.08	700	89.92	1.84	8.24	29.79	0.39	1.64	76.22	13.7

The abbreviations in the column headings are: Age=tree age in [years], Water=wet basis moisture content of wood feedstock in [%], T=highest treatment temperature in °C, FC=dry basis fixed carbon content in [%], Ash=dry basis ash content in [%], VM=dry basis volatile matter content in [%], GY=dry basis gravimetric yield in [%], D=apparent density in [g cm⁻³], TD=true density in [g cm⁻³], P=porosity (100 – 100* D/TD), and Fri=Friability in [%](described above),

The effects of the independent variables on the friability, gravimetric yield, density and fixed carbon content are given and discussed below. The ash and volatile matter contents are not discussed because the ash content is rather low overall < 3.18 %, and volatile matter content is therefore roughly proportional to fixed carbon content. The porosity was not significantly influenced by the independent variables. If two means displayed in the boxplots below are referred to as significantly different, it means that they have passed a Tukey's Honest Significant Difference test with a 95% confidence interval.

Carbonization temperature

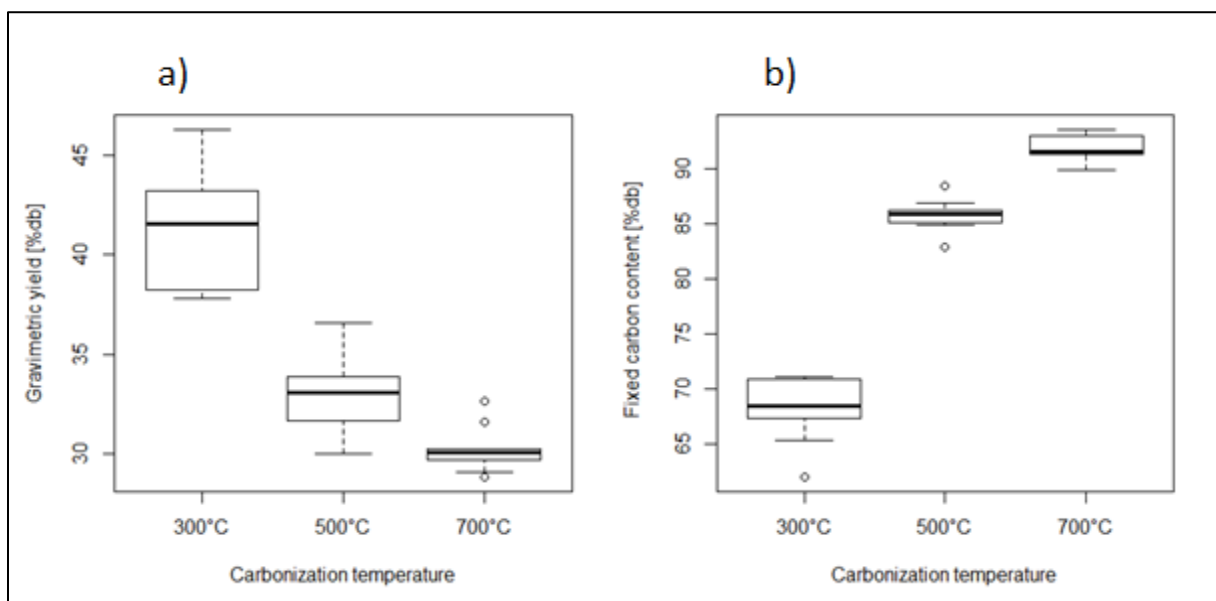


Figure 11: Gravimetric yield (a) and fixed carbon content (b) for the carbonization temperature levels, $n=9$ for all boxes.

The effect of carbonization temperature on the gravimetric yield and fixed carbon content is strong, as one would expect. The fixed carbon content being quite accurately predicted by

carbonization temperature alone is not surprising when considering that it is measured and defined as the loss of mass at certain temperatures.

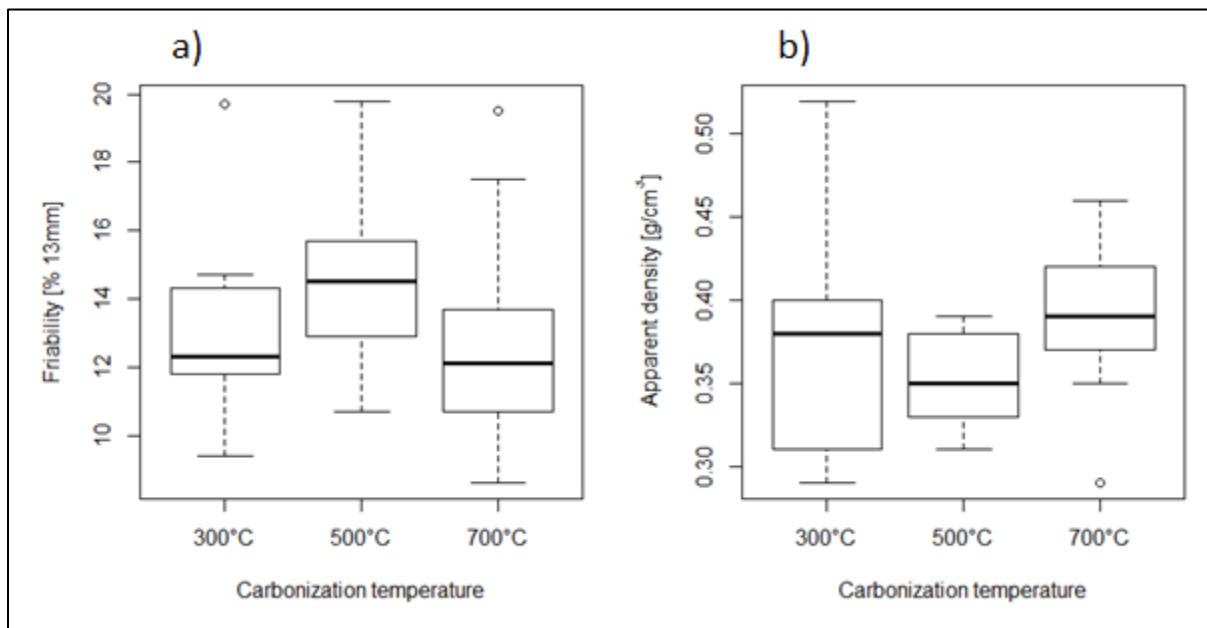


Figure 12: Friability (a) and apparent density (b) for the carbonization temperature levels, $n=9$ for all boxes.

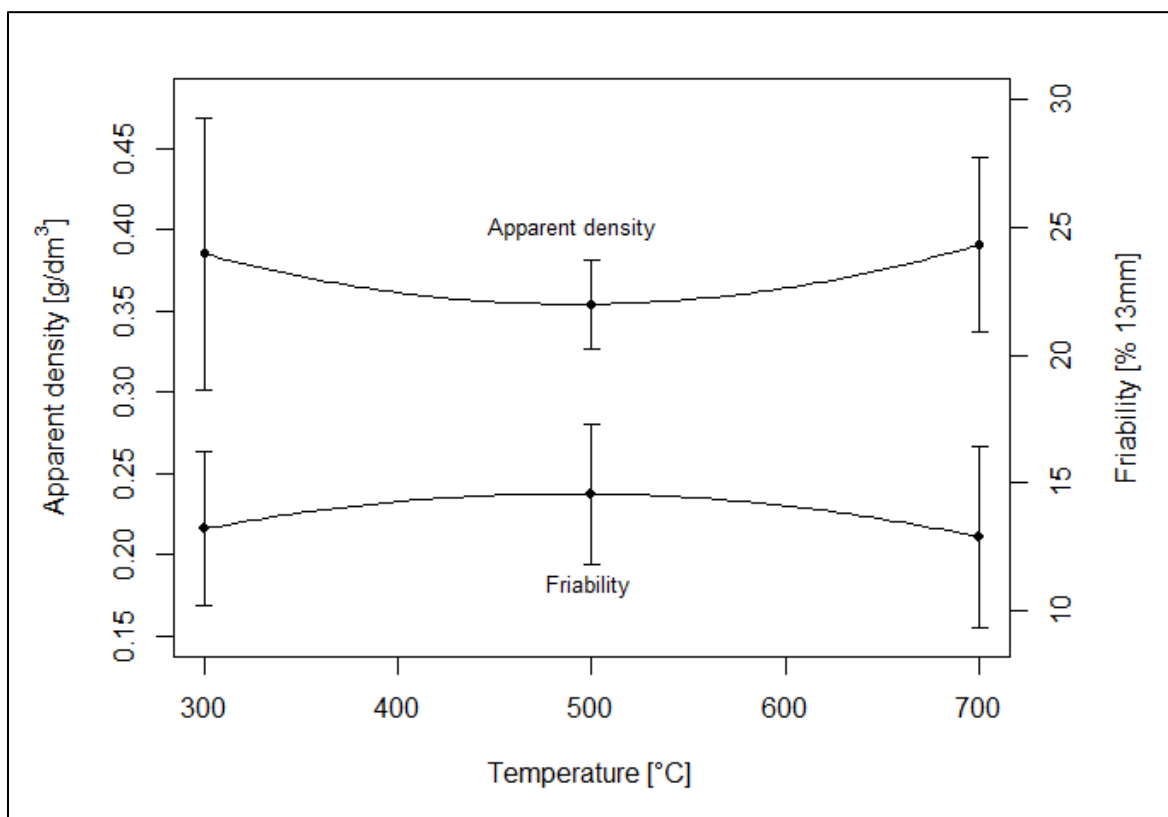


Figure 13: Apparent density and friability with standard deviations for the carbonization temperature levels.

Figure 13 shows the means and standard deviations of the bulk densities and friabilities at the different temperatures. The curves are the 2nd degree polynomial through the means.

The means for bulk density and friability at the three temperatures do not pass the Tukey's test for significance. There are however other reasons to think that the two properties are connected. Firstly, the observation that charcoal reaches a minimum density at a carbonization temperature around 500-600°C has been made by others (Blankenhorn et al., 1978; Kumar et al., 1999; Slocum et al., 1978). Similarly, other measures of mechanical strength of charcoal, like compressive strength, have been found to reach a minimum in this temperature range (Kumar et al., 1999; de Oliveira et al., 1982c; Vieira, 2009).

Since the amount of charcoal loaded into the tumbler drum has a fixed mass, the volume of the charcoal tested will vary with density. As mentioned, Oliveira found in his preliminary studies that increasing the amount of charcoal in the tumbler drum decreased the amount of fines generated, which he attributed to a cushioning effect of the additional charcoal. Following this logic alone, the friability should decrease with decreasing bulk density, given that a fixed mass of charcoal is tested. If the tumbler drum were loaded with a fixed volume of charcoal rather than mass, the peaking of friability close to 500°C would thus likely be more pronounced.

As seen below, the friability seems to be affected by both feedstock moisture content and tree age. Although the mean values should be unaffected by this, it increases the standard deviation.

Tree age

Figures 14 and 15 display the effect of tree age on the selected properties.

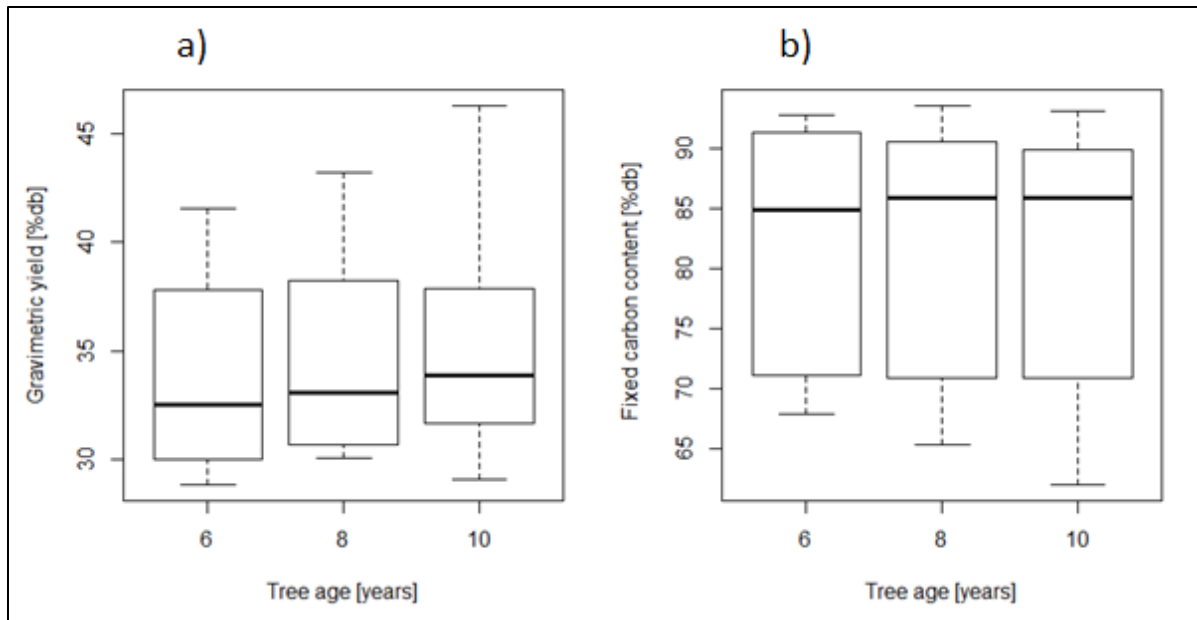


Figure 14: Gravimetric yield (a) and fixed carbon content (b) for the tree age levels, $n=9$ for all boxes.

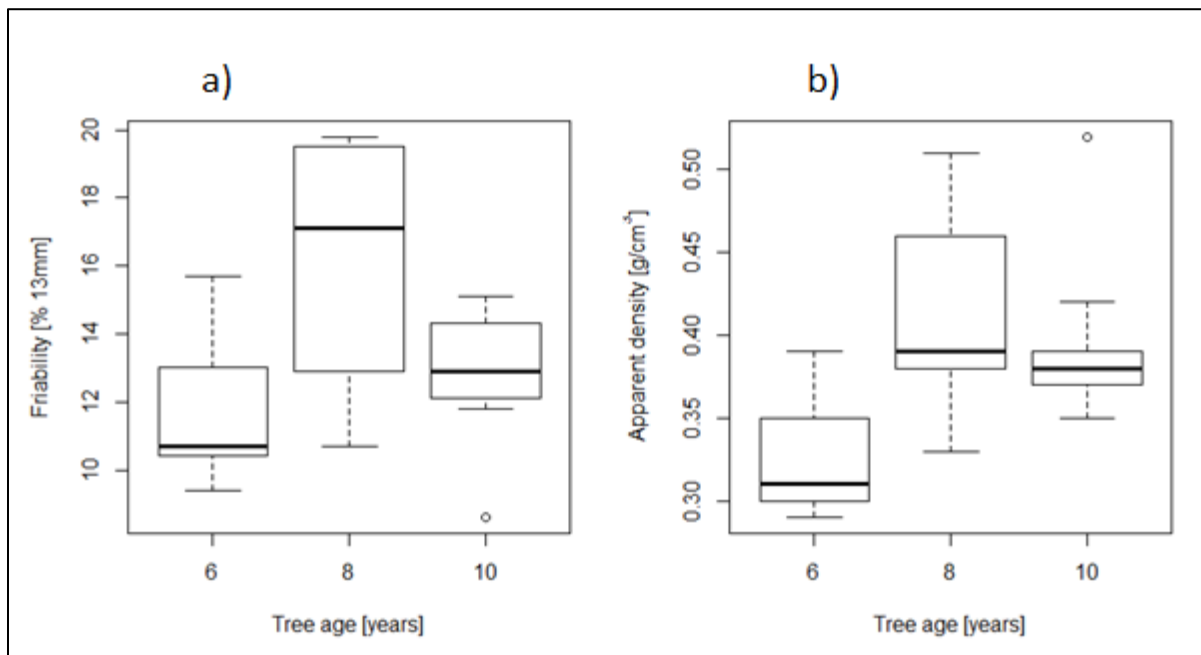


Figure 15: Friability (a) and fixed apparent density (b) for the tree age levels, $n=9$ for all boxes.

Both the friability and bulk density have significantly different means for tree ages 6 and 8 yr. The percentage increases, from age 6 to 8 yr, are 27% and 34% for bulk density and friability, respectively. This runs counter to the inverse relationship observed in figure 13, but is in some agreement with the findings of Coutinho who found both increased density and friability for increasing tree diameter (Coutinho and Ferraz, 1988). The lack of a significant increase in density from age 8 to 10 yr is however curious, considering the findings of Coutinho, and the finding of an exponential increase in density with age for *Eucalyptus grandis* from ages 0 to 10 yr (Githiomi and Kariuki, 2010). The sapwood in *Eucalyptus grandis* has also been found to be significantly denser than the heartwood in 10 year old trees, so a large portion of heartwood in the oldest trees studied by Oliveira may have off-set an increase in density from ages 8 to 10. Charcoal made from young small trees has also been reported by others to have favourable physical and mechanical properties (Antal and Mok, 1990).

Wood moisture content

The feedstock moisture contents of the samples are given in table 4 as individual measurements. They were chosen, however, to be on one of three levels of approximately <20%, 20-30%, or >30%, with nine samples on each level. Figure 16 and 17 display the values of the selected variables for each of these moisture content levels.

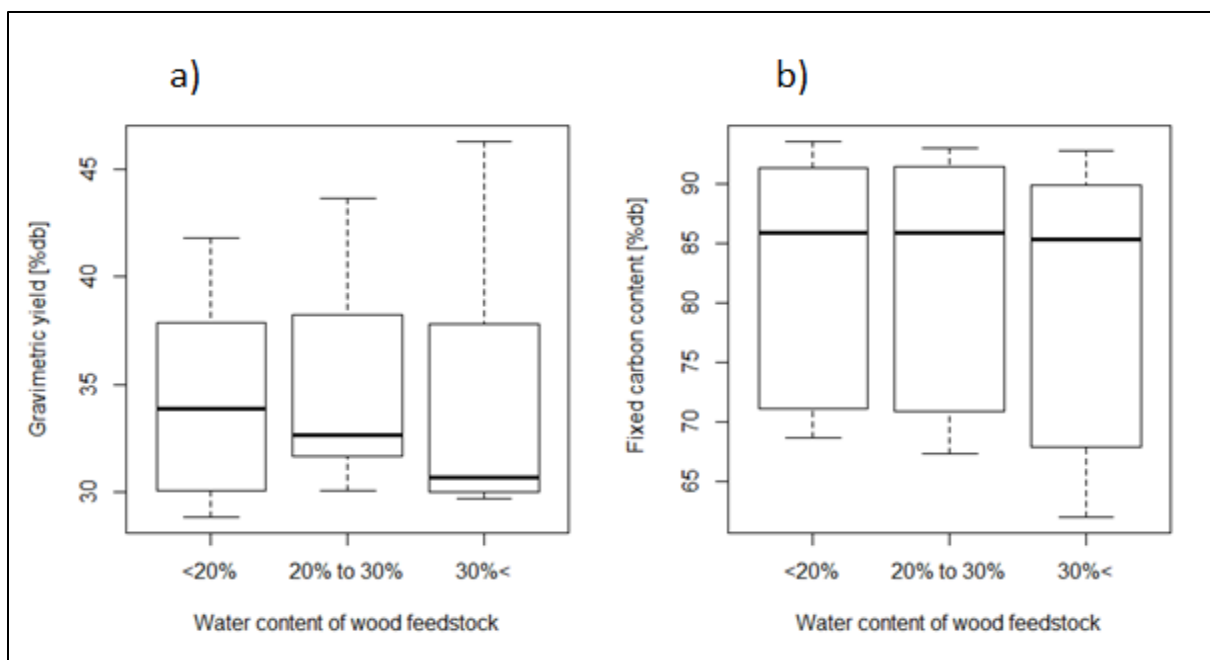


Figure 16: Gravimetric yield (a) and fixed carbon content (b) for the wood water content levels, $n=9$ for all boxes.

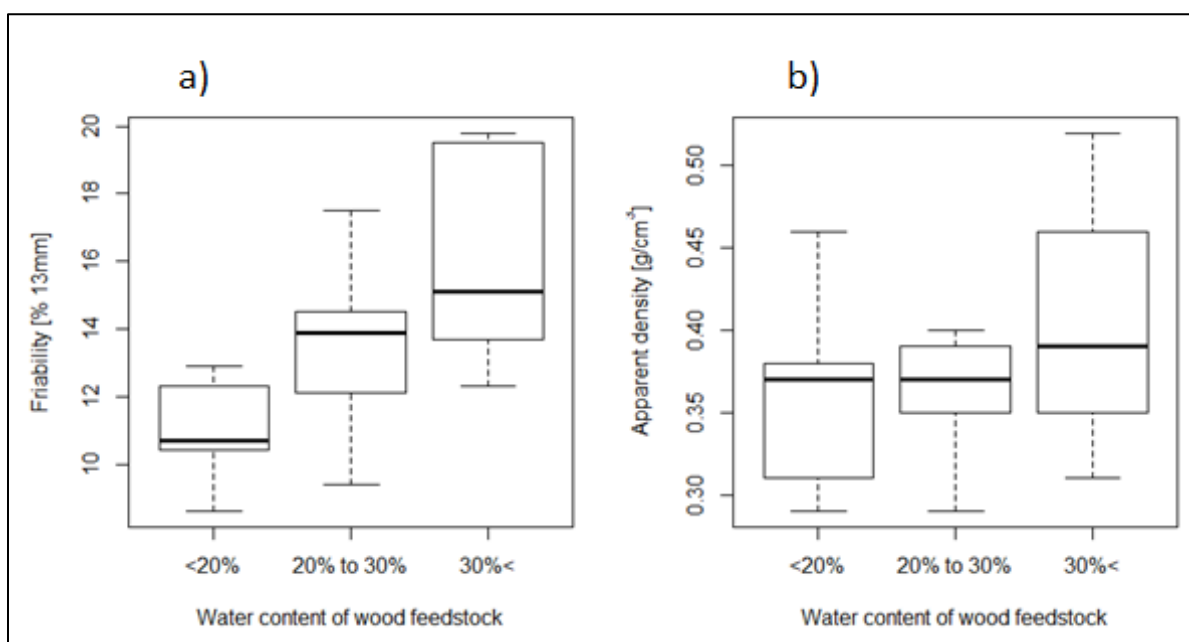


Figure 17: Friability (a) and fixed apparent density (b) for the wood water content levels, $n=9$ for all boxes.

There is a significant difference in friability between the charcoal made from the dryest wood compared to the two others, but the difference between the two wetter fractions is not

significant. Oliveira attributes the increased friability caused by moisture content in the feedstock to increased prevalence of cracks in the charcoal during the drying portion of the carbonization, which compromises mechanical strength. This indicates that the moisture content has a stronger effect on friability in the range 20-30%, while a still higher moisture content has less of an effect. A moisture content of 30% corresponds approximately to the fiber saturation point at room temperature for most woods, which may not be a coincidence (United States Department of Agriculture, 2010). As wood dries, there are abrupt changes in its mechanical strength and other properties once the fiber saturation point is reached (Grønli, 1996). An important change is shrinkage, which is often uneven along the tangential, axial and radial axes. If the drying occurs so fast so as to produce a strong moisture gradient within the wood, tension arises as the outer part of the wood shrinks around a wet core. This tension is reversed once the outer part is dry and rigid, and the inner part dries and contracts. The uneven shrinkage, and these tensions can cause both external and internal cracks (United States Department of Agriculture, 2010). The initial part of pyrolysis can be considered accelerated drying, even at relatively low heating rates, compared to the weeks or months it can take to dry green timber of 2.5 cm thickness outside (United States Department of Agriculture, 2010). It is therefore not unreasonable, that wood with a moisture content higher than the fiber saturation point could produce charcoal of compromised mechanical strength, and that this could be manifested as an increased friability. There is also a possible link between the effect of tree age and moisture content. Smaller trees have proportionally more sapwood than older trees, and sapwood is known to dry more easily than heartwood because its water conducting pathways were open and active until the tree was harvested. Since it is harder for water to escape heartwood, it may suffer more cracks and fractures during the drying stage of pyrolysis. The bulk density of the charcoal seems to be rather unaffected by feedstock moisture content, so the moisture-induced friability appears to be of a different nature than the one which is related to temperature-induced bulk density.

Model for friability

A model is now generated describing friability in terms of the three independent variables. They seem to affect the friability of the charcoal in a non-linear way. For feedstock water content, tree age and temperature, the positive effect on friability tapers off, or in the case of temperature and tree age, is reversed throughout the range of the respective variable. To account for this, the squared value of each of the variables was included. In the case of feedstock water content, the 2nd degree term yielded a p value > 0.05, so it was removed. The output of an ANOVA with the generation of coefficients with the now five variables is presented in table 5.

Table 5: Output from generation of linear model in R.

Coefficients:				
	Estimate	Std. Error	t value	Pr(> t)
(Intercept)	-6.03e+01	1.12e+01	-5.397	2.36e-05 ***
Water	2.03e-01	3.37e-02	6.031	5.51e-06 ***
Temp	3.51e-02	1.68e-02	2.083	0.0497 *
Temp^2	-3.60e-05	1.67e-05	-2.150	0.0433 *
Age	1.55e+01	2.69e+00	5.776	9.85e-06 ***
Age^2	-9.49e-01	1.68e-01	-5.665	1.27e-05 ***

Significance codes: 0 '***' 0.001 '**' 0.01 '*' 0.05 '.' 0.1 ' ' 1				
Residual standard error: 1.639 on 21 degrees of freedom				
Multiple R-squared: 0.7735, Adjusted R-squared: 0.7196				
F-statistic: 14.34 on 5 and 21 DF, p-value: 3.62e-06				

As can be observed in table 5, the temperature terms are by far the least significant contributors to the friability out of the independent variables.

The coefficients in table 5 yield the following equation for friability;

$$F(T, A, W) = -60.31 - 3.597 \cdot 10^{-5} \cdot T^2 + 0.035 \cdot T - 0.9488 \cdot A^2 + 15.52 \cdot A + 0.2033 \cdot W$$

where F is friability % <13 mm, T is carbonization temperature in °C, A is tree age in years, and W is % feedstock moisture content, and

$$300 \leq T \leq 700 \quad 6 \leq A \leq 10 \quad 14 \leq W \leq 47$$

In this model, the moisture term is linear, so any increase in moisture content of the wood increases friability. The age term has two local minimums in the range of A, A=6 being the smallest. A=8.17 is the age which yields the highest friability. Similarly, examining the temperature terms, T=300 yields the lowest friability, where after it increases to a peak at T=487.

This apparent temperature of maximum friability, inconveniently corresponds well with the peak temperatures in internally heated charcoal kilns like the Missouri kiln, where the temperature is governed by the exothermicity of the pyrolysis process itself. To make the charcoal less friable through a peak temperature increase, external heating would be required. The marginal decrease in friability one might obtain, would perhaps be off-set by the increased cost of production.

Since fixed carbon content is quite accurately determined by carbonization temperature, the temperature of maximum friability can be used to calculate the fixed carbon content of maximum temperature as shown in figure 18. However, the p-values of the temperature terms in table 5 indicate that temperature is the poorest predictor out of the independent variables. Fixed carbon content is poorer still, illustrated in figure 19.

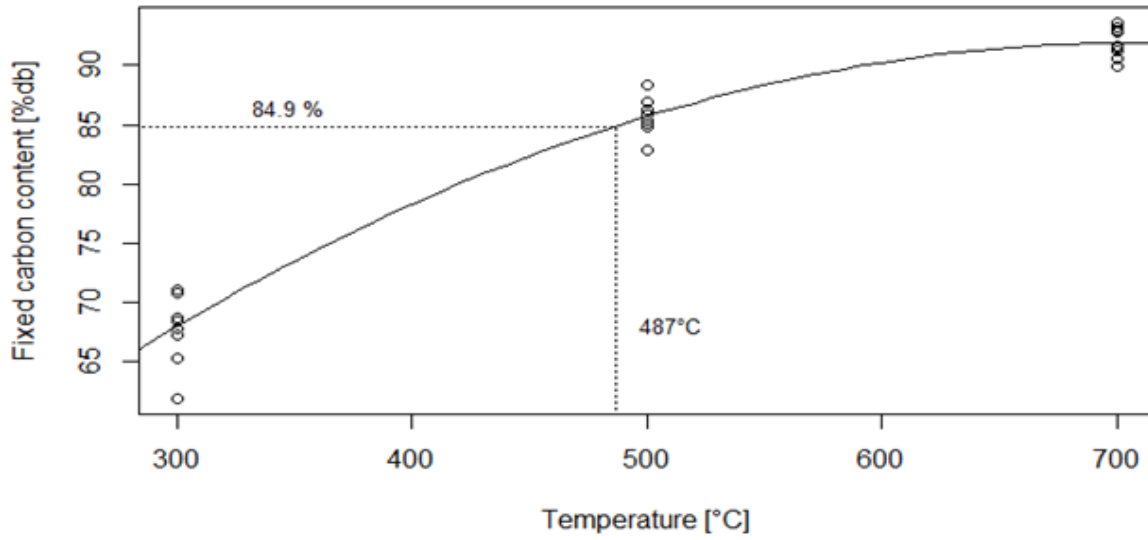


Figure 18: Fixed carbon content as a function of temperature. The dotted lines are temperature and corresponding fixed carbon content at maximum friability.

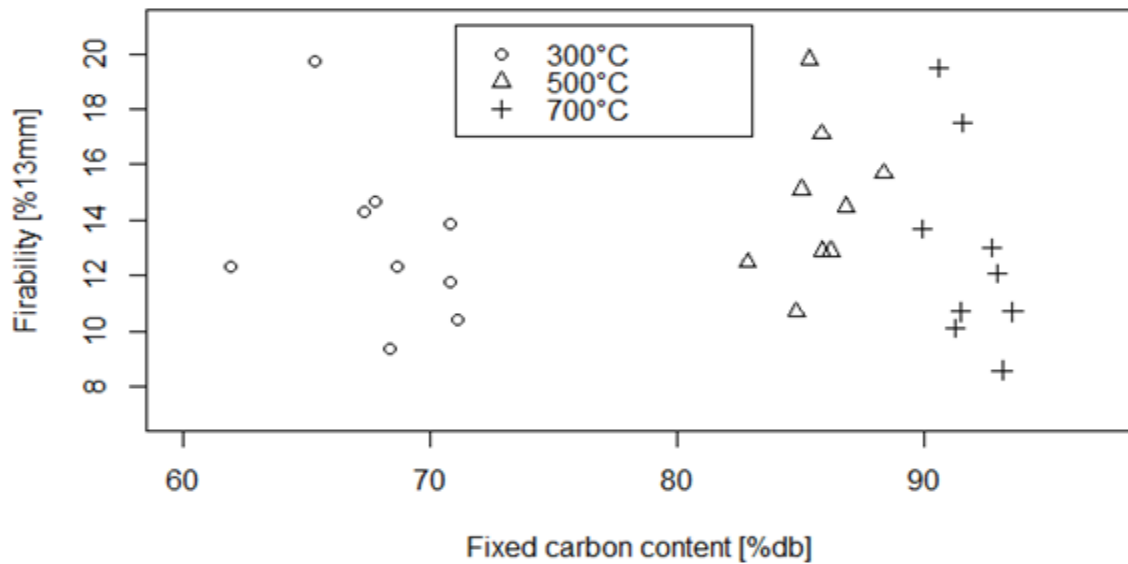


Figure 19: Friability vs fixed carbon content

Principal component analysis friability

The data in table 4 is now submitted to a principal component analysis to uncover correlations within all the variables, and to have a visualization of them. Since the variables have different units, the Pearson correlation matrix is used in constructing the principal components. This matrix is presented in table 6 where correlations with absolute values ≥ 0.4 are in bold.

Table 6: Pearson correlation matrix.

	Age	Temp	FC	Ash	VM	D	GY	Fri	Water	TD	P
Age	1.00	0.00	-0.02	-0.44	0.05	0.50	0.16	0.12	-0.10	0.09	-0.42
Temp	0.00	1.00	0.95	0.41	-0.95	0.04	-0.87	-0.04	0.01	0.88	0.45
FC	-0.02	0.95	1.00	0.37	-1.00	-0.11	-0.95	-0.02	-0.04	0.74	0.52
Ash	-0.44	0.41	0.37	1.00	-0.42	-0.33	-0.37	-0.15	-0.22	0.23	0.41
VM	0.05	-0.95	-1.00	-0.42	1.00	0.13	0.95	0.03	0.05	-0.73	-0.54
D	0.50	0.04	-0.11	-0.33	0.13	1.00	0.20	0.40	0.30	0.17	-0.83
GY	0.16	-0.87	-0.95	-0.37	0.95	0.20	1.00	0.00	0.01	-0.65	-0.56
Fri	0.12	-0.04	-0.02	-0.15	0.03	0.40	0.00	1.00	0.58	-0.09	-0.40
Water	-0.10	0.01	-0.04	-0.22	0.05	0.30	0.01	0.58	1.00	-0.03	-0.30
TD	0.09	0.88	0.74	0.23	-0.73	0.17	-0.65	-0.09	-0.03	1.00	0.40
P	-0.42	0.45	0.52	0.41	-0.54	-0.83	-0.56	-0.40	-0.30	0.40	1.00

Table 6 indicates significant correlation among several of the variables. This is confirmed through the PCA. By the Kaiser criterion (eigenvalues >1), the first three principal components are sufficient. This implies that the 11-dimensional space of variables can be reduced to a 3-dimensional one while retaining sufficient information to explain 81.9 % of the variance (table 7).

Table 7: Importance of components

Importance of components:	Comp.1	Comp.2	Comp.3
Standard deviation	2.261	1.581	1.181
Proportion of Variance	0.465	0.227	0.127
Cumulative Proportion	0.465	0.692	0.819

Table 8: Loadings of variables on principal components

Loadings:	Comp.1	Comp.2	Comp.3
Age		-0.349	0.556
Temp	-0.411	-0.206	
FC	-0.419	-0.153	
Ash	-0.236	0.218	-0.199
VM	0.424	0.134	
Dens	0.133	-0.534	0.156
GY	0.409		
Fria		-0.397	-0.474
Water		-0.329	-0.596
Tru	-0.341	-0.228	0.183
Por	-0.315	0.365	

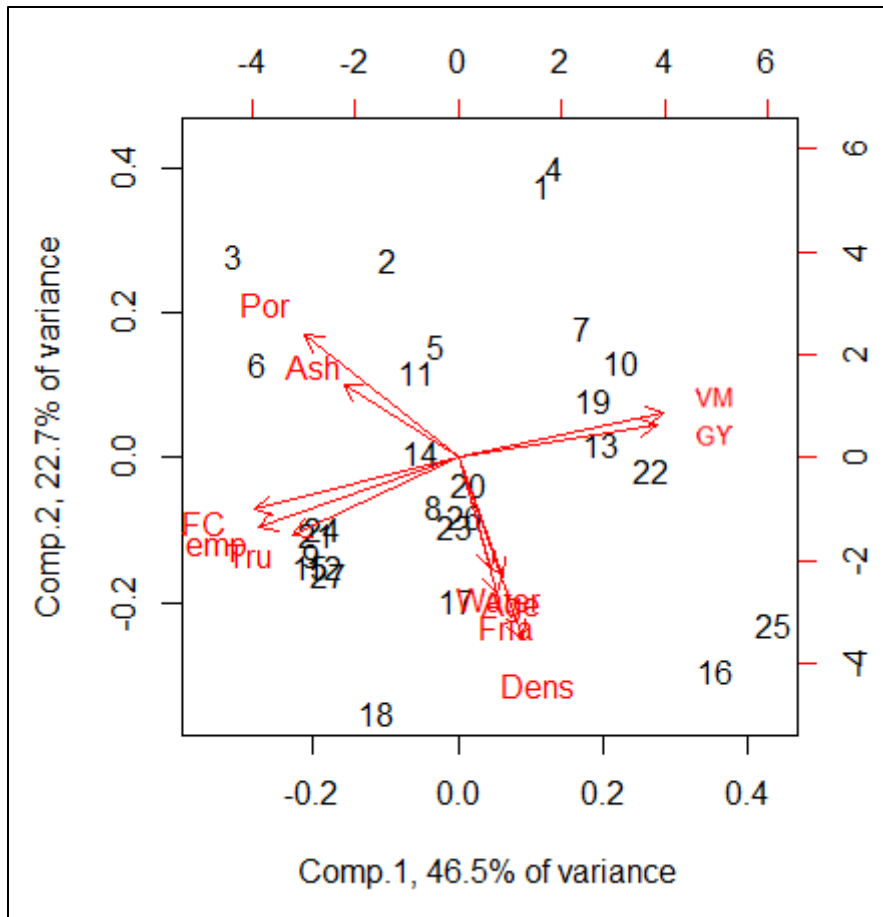


Figure 20: Biplot

The biplot of the first two principal components is presented in figure 20, providing a visualization of the loadings of the variables on the first two principal components. The variables have been converted to vectors of equal length. The vectors in figure 20 are projections of these vectors onto the plane defined by the two first principal components. A longer projection, like the one for VM, indicates that the variable is well expressed by the first two principal components. The angle between two vector projections reflects the degree to which they correlate. Angles of 0 and 180° indicate positive and negative correlation respectively, while orthogonal vector projections indicate little correlation. Any correlation indicated by the angles is less certain for shorter vector as these can be better expressed by other principal components.

The biplot reveals four predominant directions of the projections of the variable vectors on the plane defined by the two first principal components. The variables that are approximately horizontally aligned are well expressed by the first principal component. The independent variable temperature is among these. This can be interpreted as temperature being the major

cause of change in these properties. Nearly orthogonal to these are the cluster of variable most vertically aligned. It is hard to read from the plot, but these are Age, Water, Fria and Dens. They appear to be nearly uncorrelated with temperature and the strongly temperature determined properties. Fria and Water are well aligned but have short projections in the biplot. Both do, however, have similar strong loadings on the third principal component. The choice of tree age, wood moisture and temperature as independent variables explaining friability appears to have been a good good, in revealing that the two former turned out to be good predictors of friability, and the latter less so than one might expect.

Friability varying with tree diameter

Coutinho and Ferraz (1988) studied the effect of carbonization temperature and tree diameter on friability of charcoal from *Eucalyptus saligna*, which is closely related to *Eucalyptus grandis* used in Oliveiras studies. The wood used was nine year old, and harvested from a plantation in northern Brazil. After harvesting, their diameter at breast height (1.3m), was measured and they were sorted into five diameter classes. D1 denotes the smallest diameter, 7.5 to 10 cm, increasing through D5, measuring 17.5 to 20 cm. They employed virtually the same tumbler test specifications as Oliveira: same size drum, number of rotations, mass of charcoal per run and same upper size limit for fines. The rotation speed was slightly slower, at 30 RPM. The granulometry of the charcoal was not reported, but prior to carbonization, the wood was cut into blocks of height and width of 4 cm and length equal to the diameter of the tree, 10 to 20 cm. Heating rate was $1.67\text{ }^{\circ}\text{C min}^{-1}$, and residence time at target temperature was not reported. Prior to carbonization, the wood was slowly dried to reach a moisture content of 10% to avoid cracks, and then further dried in a drying chamber maintaining $105\pm 3\text{ }^{\circ}\text{C}$. The results are presented in figure 21.

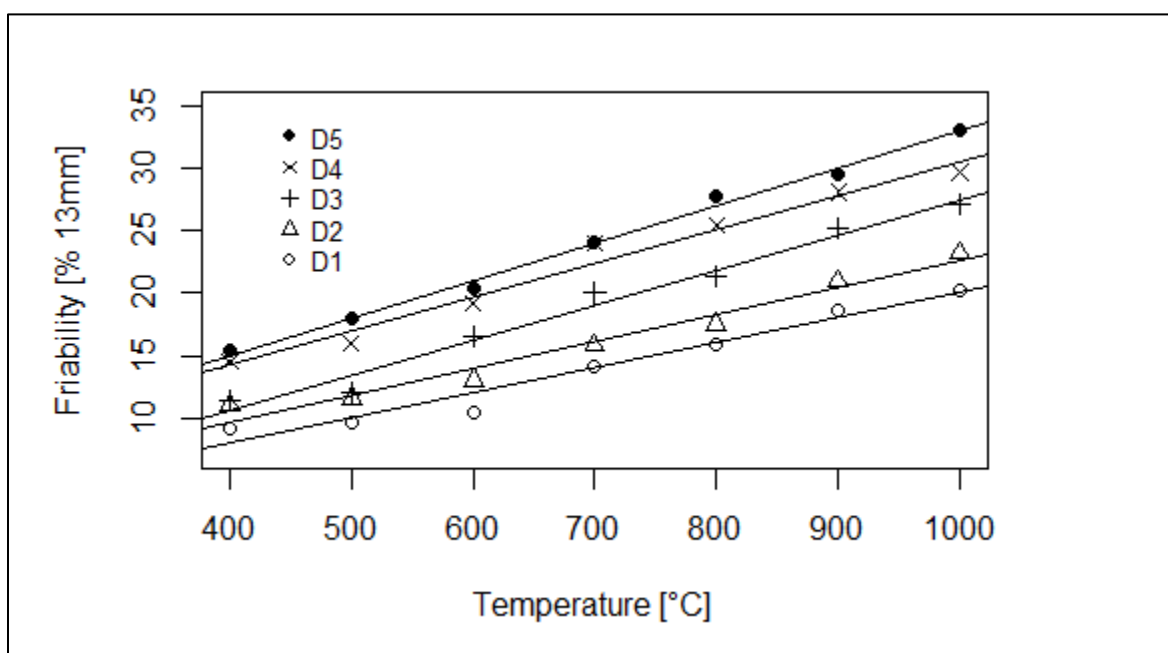


Figure 21: Friability varying with carbonization temperature and tree diameter.

The friability was found to strictly increase with both carbonization temperature and diameter. The decrease of friability from 500°C to 700°C found by Oliveira, is not apparent for any diameter class. The granulometry of the samples entering the tumbler was not explicitly reported, but due to the slow and thorough drying, and low heating rate, minimal cracking of the samples during carbonization is likely. They therefore likely entered the tumbler drum in their elongated shape. Eucalyptus wood has been found to shrink roughly linearly from about 65% volumetric yield at 300°C to 45% at 1000°C (Kumar et al., 1999). Assuming radial, tangential and axial shrinkage like that found for Oak (E. A. McGinnes et al., 1971), or even the same shrinkage in all three directions, the cross-sectional area of the elongated samples would decrease more than the length, increasing the likelihood of breaking. An increased friability may thus be measured with increasing temperature because of the way shrinkage affects elongated pieces of charcoal.

Coutinho reported a density of the charcoal roughly proportional to the density of the wood. The density also increased radially from the pith to the bark for all the samples. The density close to the pith was similar across the diameter classes, while the density just beneath the bark increased with increasing tree diameter. This means that the samples from higher diameter trees were denser, on average. This result agrees with the finding made by Oliveira that both friability and bulk density increase with tree age, if one assumes tree age and tree diameter can be said to be proxies for the same tree property, calling it for instance “tree size”.

The five smaller studies

The friability of charcoal as measured in tumbler tests from the five last sources is now presented (de Assis, 2007; Gomes da Silva et al., 2007; Lana, 2012; Nouni et al., 2014; da Silva et al., 2014). Even though there are variations in the experimental settings across the them, the friability has been by tumbler drum tests in all of them, and the change granulometry is measured after treatment, and presented as a percentage of the initial weight. Since there are differences in the experimental settings across the sources, the friability values obtained cannot be directly compared. However, they are assumed to be measuring the same property of the charcoal, so that a charcoal scoring a high friability in one test would score proportionally high in the others. Friability measurement specifications for the sources are given in table 9.

Table 9: Friability standard applied, and cut off size for fines (Size reduction measured according to NBR 7416/84 of ABNT, which involves several cut off sizes for fines)*

Source	Standard applied	Size fines
Nouni et al., (2016)	MB 1375/80 of ABNT	<3mm
Silva et al., (2007)	MB 1375/80 of ABNT	<20 mm
de Assis, (2007)	MB 1375/80 of ABNT	NA
da Silva et al., (2014)	MB 1375/80 and NBR 8740/85 of ABNT	<10 mm
Lana, (2012)	NBR 8740/85 of ABNT	Several*

In addition to friability, the only other property of the charcoal reported in all the sources is the dry basis fixed carbon content. The other variables present in more than one of the sources are ash content, apparent density and gravimetric yield. The data is presented in table 10.

Table 10: Charcoal properties

Source	Feedstock	Temperature [°C]	Fixed carbon [%db]	Ash [db%]	Apparent density [g cm ⁻³]	Gravimetric yield [%]	Friability [%]
Noumi et al., (2016)	<i>Eucalyptus camaldulensis</i>	350	60.44	n/a	0.4	48.02	6.35
		350	48.77	n/a	0.32	47.97	8.74
		600	87.15	n/a	0.41	34.35	5.55
		600	87.02	n/a	0.29	34.18	5.82
	<i>Eucalyptus urophylla</i>	350	54.77	n/a	0.35	50.73	3.93
		350	50.55	n/a	0.3	46.26	3.37
		600	90.22	n/a	0.34	32.11	6.2
		600	87.27	n/a	0.32	30.13	6.09
da Silva et al., (2007)	Macaranduba	n/a	74.49	0.8	0.55	n/a	26.6
		n/a	71.35	0.7	0.52	n/a	32.6
	Sapucaia	n/a	72.66	1.3	0.56	n/a	30.2
		n/a	73.58	2.5	0.49	n/a	27.6
	Timborana	n/a	74.02	1.5	0.38	n/a	12
		n/a	68.29	1.4	0.39	n/a	14.67
de Assis, (2007)	<i>Eucalyptus</i> sp.	n/a	75.39	0.17	0.39	36.07	16.98
		n/a	80.52	0.43	0.4	28.61	13.03
		n/a	70	0.12	0.36	36.42	17.79
		n/a	73.55	0.22	0.41	33.83	13.03
		n/a	73.32	0.11	0.43	28.69	13.01
		n/a	76.49	0.11	0.43	35.63	13.61
		n/a	71.95	0.12	0.43	34.9	13.2
		n/a	74.18	0.22	0.45	29.3	12.04
		n/a	70.78	0.05	0.48	32.02	17.98
		n/a	71.75	0.24	0.37	32.87	9.51
da Silva et al., (2014)	Cardeiro	n/a	71.47	1.55	n/a	n/a	3.8
	Cedrinho	n/a	69.54	1.67	n/a	n/a	5.81
	Louro	n/a	71.13	0.22	n/a	n/a	2.7
	Piquiarana	n/a	67.72	1.5	n/a	n/a	5.28
Lana, (2012)	<i>Eucalyptus</i> sp.	n/a	81.7	0.77	n/a	30.1	52.3
		n/a	78.1	0.73	n/a	31.6	49
		n/a	75.9	0.66	n/a	30.9	43.4
		n/a	82.7	0.6	n/a	32.6	57
		n/a	77.8	0.5	n/a	31.8	59.6
		n/a	81.5	0.72	n/a	31.7	61.2

Except in Noumi et al., (2016), the carbonization of the wood was done in internally heated kilns where the temperature was regulated, initially by combustion of part of the feedstock,

and then by the exothermicity of the pyrolysis process. The peak temperature for these was thus not precisely controlled or measured. De Assis,(2007) estimated the peak temperature of her carbonization to have been approximately 450°C based on the fixed carbon content of the charcoal. Since the production methods of the other sources, for which the temperature is unknown, is similar, and they have a comparable fixed carbon content to de Assis' charcoal, it appears reasonable to assume a similar peak temperature in them as well.

Standardized plots of friability

To investigate if there is a connection between friability and the other properties of the charcoal, the data has been standardized. All the values, where they are available, are transformed to a z-value reflecting the deviation of the value from the mean of the variable in its respective source. The calculation of the first friability value from Noumi is given below as an example.

$$n = 6, x = 6.35$$

$$\mu = \frac{\sum_1^n F}{n} = 5.76$$

$$\sigma = \sqrt{\frac{\sum_1^n (\mu - x)^2}{n - 1}} = 1.63$$

$$z = \frac{x - \mu}{\sigma} = 0.36$$

Where μ and σ are the mean and standard deviation of the friability values of Noumi, x is the value to be transformed, and n is the number of friability values of Noumi. Below are the plots of the standardized values. Only the top left plot has values from all the samples, while the others include only data where it is available. The units of both axes in all four plots are standard deviations from the mean.

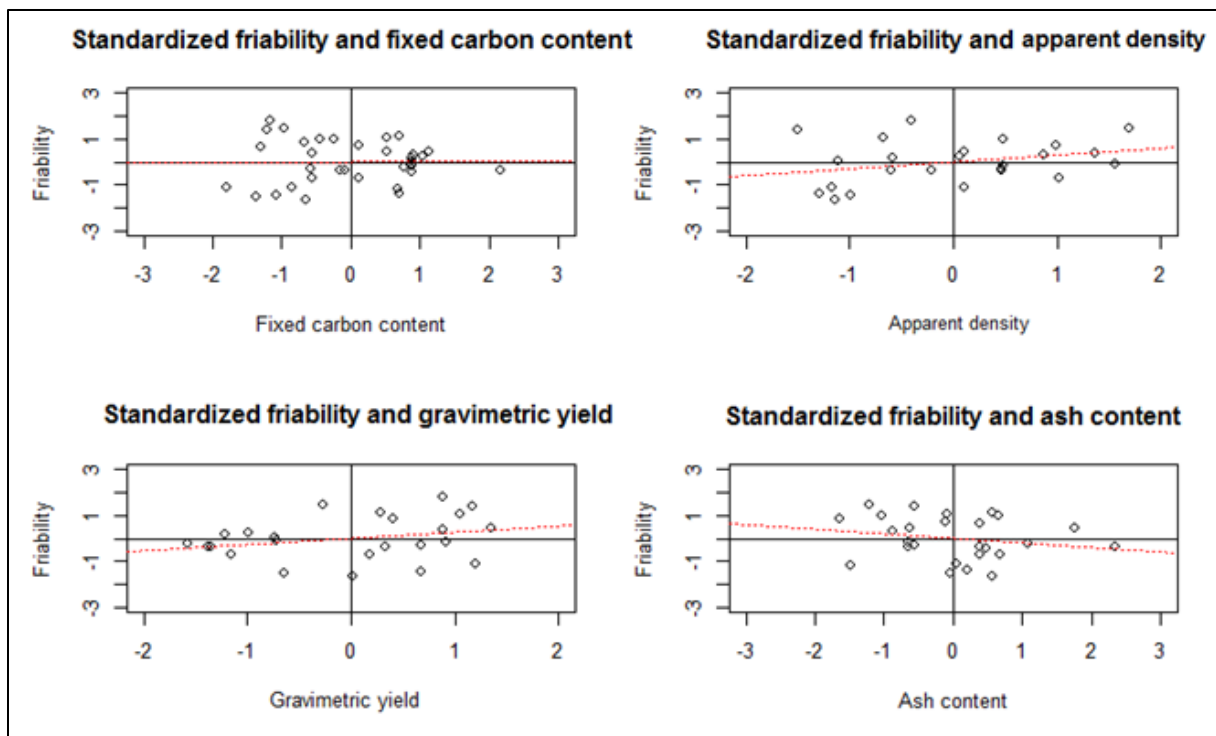


Figure 22: Standardized friability versus standardized fixed carbon content, apparent density, gravimetric yield and ash content.

A positive or negative correlation between the plotted variables would be indicated by a clustering of samples in the upper right and lower left quadrants or the upper left and lower right quadrants respectively. This is not observed for any of the four variables. Indeed, the fixed carbon content plot has an approximately horizontal trendline, indicating no correlation. Although the red best fit lines may indicate some weak trend in three of the plots, their R^2 -values are all <0.09 , and thus highly insignificant.

Comparative plots data

To reveal how the data from each source influence the trend, or lack thereof in figure 22, the values from table 10 are plotted against friability in figures 23 through 26. In these plots, the data from de Oliveira et al., (1982a) has been included for comparison. The lines are the best fit linear regression lines. It should be noted that the y-axes in these plots serve only to compare points with the same symbols, because the testing specifications for friability vary among the sources.

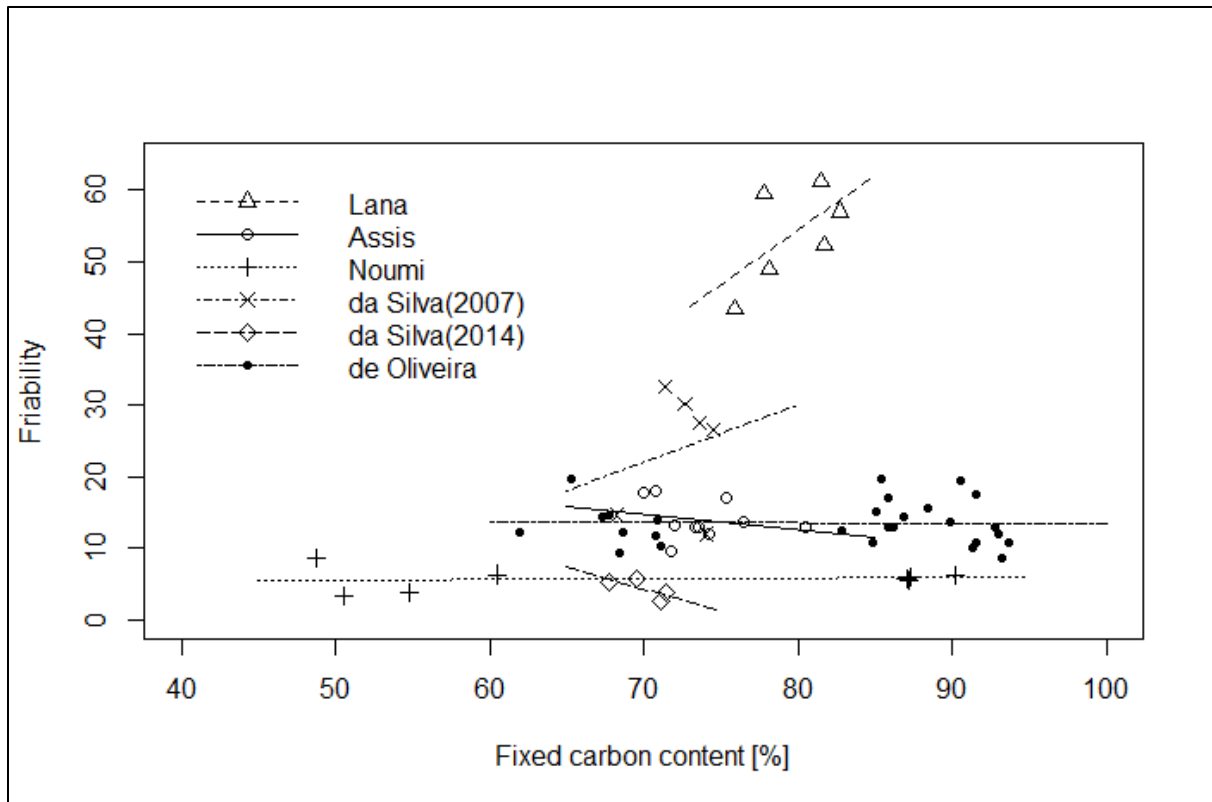


Figure 23: Friability vs fixed carbon content

From figure 23 it can be seen how the near horizontal line was generated in the top left plot in figure 22. Where the sample size and or fixed carbon content range is wide, Noumi and de Oliveira, the trend line has a slope of nearly zero. For the other sources, the sample size is small and the range of fixed carbon content narrow. This may cause an appearance of a trend that would vanish if one or both of sample size and fixed carbon range were increased. The temperature of maximum friability, found from the model based on table 5, of 487°C is close to the estimated temperature for these four sources, so an average slope of approximately zero, could be expected based on this. The same applies to Noumi since the average temperature employed was 475°C. Despite this, fixed carbon content being a very poor indicator of friability in the temperature range 300-700°C is found again.

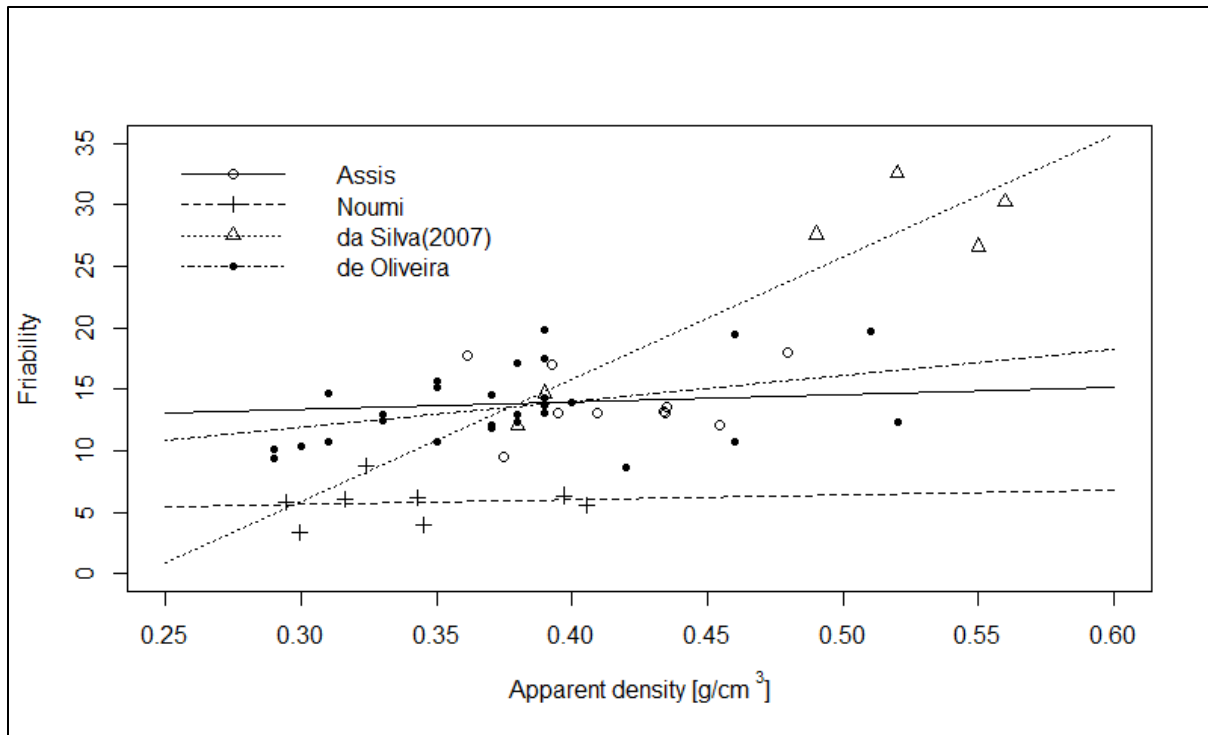


Figure 24: Friability vs apparent density

In figure 24, all four trendlines have positive slopes, indicating that denser charcoal is more friable. Given what was found from figure 13 and figure 15 a and b, the slightly positive trend found in the data from de Oliveira et al. may be a result of the effect of tree age. The steepest trend, may again be a product of the small sample size of six in da Silva et al., (2007), but also that they are from three different wood species. The apparent density of charcoal is known to be highly dependent on and roughly proportional to, that of the wood precursor (Antal and Grønli, 2003).

The following two points may also be hypothesized to contribute to the observed trends. Firstly, the point mentioned in the discussion of figure 13, namely that higher density leads to a lower volume of charcoal per tumbler drum run, and the cushioning effect is thus smaller. Secondly, denser particles will be heavier, given the fixed granulometry of the charcoal entering the tumbler drum. They will thus attain a higher momentum than their lighter counterparts and collide more forcefully with the inside of the drum and neighbouring particles.

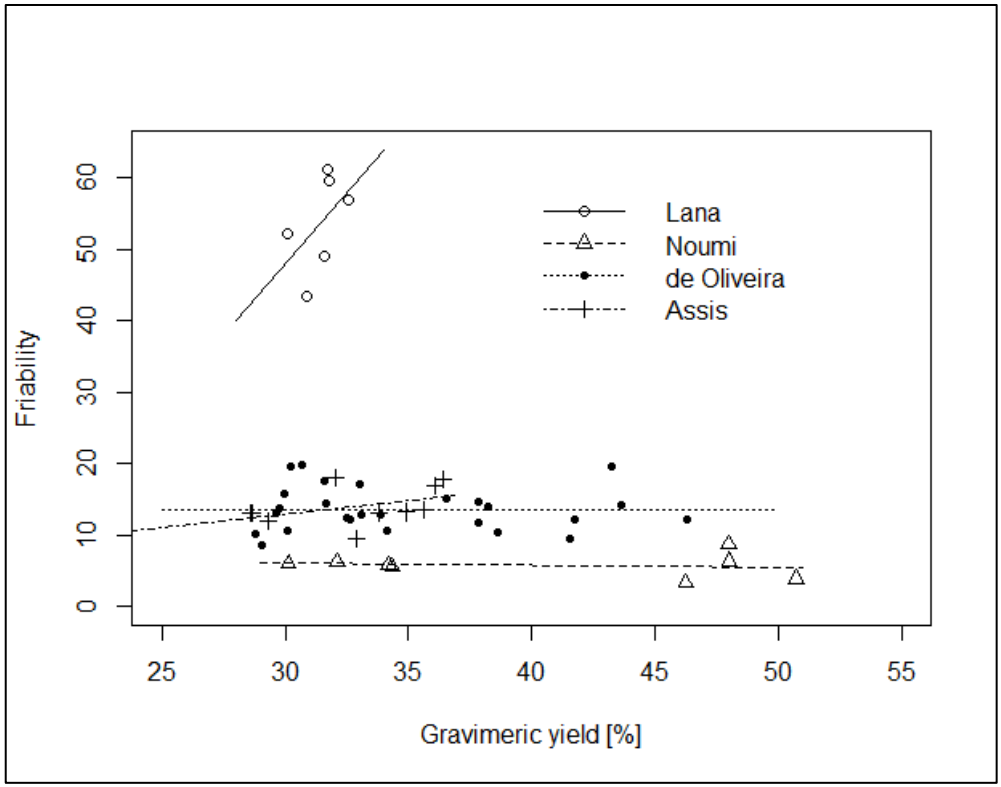


Figure 25: Friability vs gravimetric yield

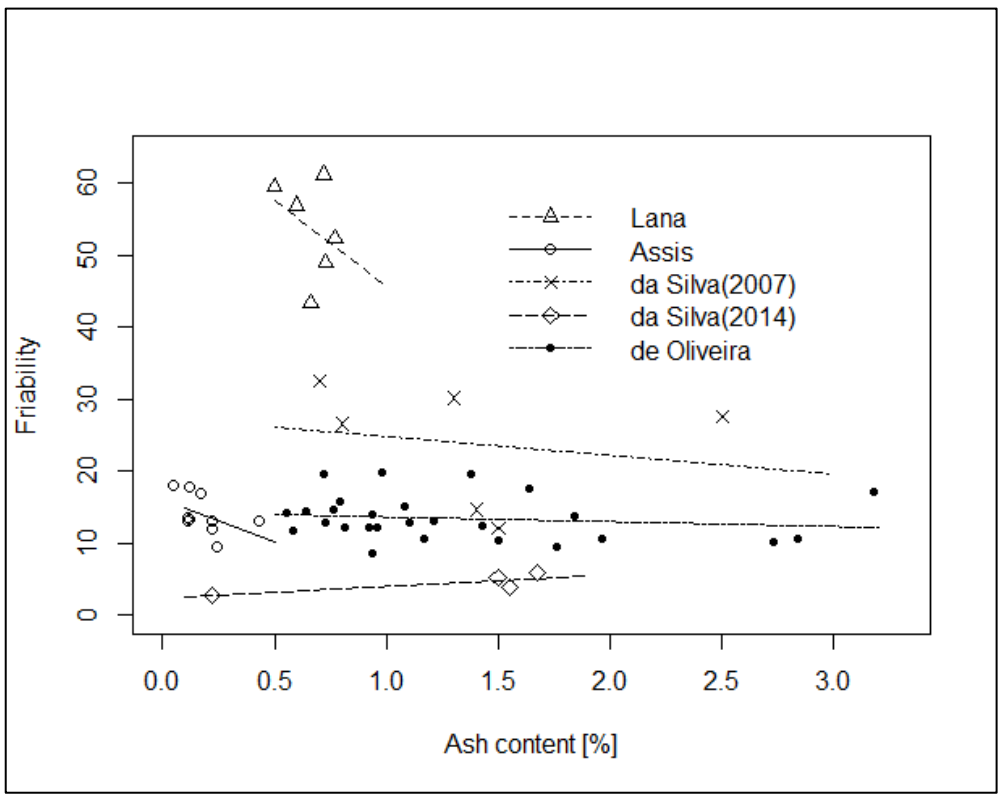


Figure 26: Friability vs ash content

Similarly to what was found in the case of fixed carbon content, only the data set with a small sample size and narrow range of values on the x axis show any trend to speak of in figure 25. The same is observed for the ash content (figure 26), which is low overall, as can be expected of wood charcoal barring any contamination, some specific wood species or exceedingly high carbonization temperatures.

Comparison of data from the different sources proved challenging for tumbler drum test, since a common standard was not strictly adhered to by any two sources. Additionally the small sample sizes in the sources and the limited amount of properties analysed, except for de Oliveira et al., (1982a), made drawing conclusions with confidence difficult.

It has been claimed that the friability of charcoal increases with fixed carbon content, or decreases with volatile matter content, which amounts to the same (FAO Forestry Department, 1987; Misginna and Rajabu, 1996). The findings from all the sources analysed above, where fixed carbon content was measured, suggest that very little can be known of the friability of charcoal from knowing its fixed carbon content.

Without the well-constructed experiments done by Oliveira et al, drawing any conclusion from this section on friability would be difficult.

Grindability

Although the HGI testing is different from tumbler testing, there are reasons to believe that it is correlated to some not insignificant degree with other mechanical properties of the pyrolyzed biomass. Mechanical properties like tumbler drum friability, compressive strength, impact strength and dynamic elastic modulus have been found to respond similarly to changes in carbonization temperature (Antal and Grønli, 2003; Kumar et al., 1999; de Oliveira et al., 1982c). The stresses a substance is subjected to in a hardgrove mill must be, at least in part, some combination of those. The HGI has also been found to correlate highly with values obtained when the ball mill was replaced by a small tumbler drum containing steel balls (Terchick et al., 1963). It can therefore be reasonable to consider HGI a measure of mechanical strength.

The Hardgrove Grindability Index (HGI) is a well-established standard for measuring the grindability of a substance (Hardgrove, 2015). The substance with a given particle size is ground in a Hardgrove ball mill, and the reduction in particle size after milling yields a unit less number.

$$HGI = 13 + w \cdot 6.93$$

Where w is the weight of the initial sample passing through a sieve, normally of mesh size 74 μm , after milling. A low HGI indicates a hard substance with low grindability. The calibration of the equipment is done by testing substances of known HGI. The standard was developed to determine the grindability of coal for use in pulverized coal power plants. It has since been applied to other substances like torrefied or pyrolyzed biomass to assess their potential for replacing coal in said power plants. Because of the fibrous structure of wood and woody biomass, they are not easily grindable. Especially in ball mills, like the hardgrove mill, the fibres tend to get flattened rather than broken. Torrefaction breaks depolymerizes the structural components of the wood rendering it more brittle.

In the following, data from three studies reporting the grindability of torrefied biomass is presented (Bridgeman et al., 2010; Ohliger et al., 2013; Raimie H. H. et al., 2013). All the biomass investigated were wood chips, except for *Mischantus*. *Mischantus* is a genus with various species in the grass family. Although the species of *Mischantus* investigated by Bridgeman was not stated, it was presumably *Mischantus giganteus*, a sterile hybrid species grown as an energy crop in the EU.

Table 11: Torrefied biomass properties

Source	Biomass	Experiment settings				Measured values				
		Temp [°C]	HR [°C/min]	RT [min]	PS [mm]	GY [%db]	Ash [%db]	FC [%db]	VM [%db]	HGI
Bridgeman et al., (2010)	Willow	290	Instant	10	<10	81.6	2.15	23.82	74.03	24.00
		240	Instant	60	<10	89.5	1.53	21.04	77.43	0.00
		240	Instant	10	>20	97.7	1.23	15.02	83.74	10.00
		290	Instant	60	>20	66.9	1.84	29.83	68.34	51.00
	Miscanthus	290	Instant	10	<4	75.7	1.43	33.33	65.24	26.00
		240	Instant	60	<4	87.2	1.33	20.47	78.20	1.00
		240	Instant	10	>10	96.9	1.23	15.38	83.38	11.00
		290	Instant	60	>10	60.3	1.95	36.45	61.60	79.00
Ohliger et al., 2013;	Beech	280	Instant	40	>10	70.52	0.88	28.07	71.20	49.00
		270	Instant	40	>10	76.49	0.99	22.80	76.43	36.00
		290	Instant	40	>10	62.98	0.92	32.46	66.81	73.00
		300	Instant	40	>10	51.64	1.49	42.03	56.82	122.00
		280	Instant	20	>10	77.56	0.90	24.58	74.72	37.00
		280	Instant	60	>10	65.82	0.95	30.84	68.43	67.00
		280	Instant	40	>10	67.39	0.96	30.83	68.40	64.00
		280	Instant	40	>10	73.78	0.85	26.50	72.76	40.00
Raimie H. H. et al., 2013	Willow	270	10	30	10-50	68.76	0.50	26.20	73.80	64.60
		290	10	30	10-50	56.21	1.10	36.80	63.20	86.40
	Eucalyptus	270	10	30	10-50	67.62	1.60	32.10	67.90	38.90
		270	10	60	10-50	56.66	2.00	28.80	71.20	46.80
		290	10	30	10-50	50.61	2.20	39.70	60.30	79.60
	Hardwood mix	270	10	30	10-50	73	1.00	27.80	72.20	43.30
		270	10	60	10-50	71.6	1.60	28.00	72.00	41.80
		290	10	30	10-50	59.15	2.10	35.40	64.60	63.30
	Softwood mix	270	10	30	10-50	79.53	0.10	20.30	79.70	41.50
		270	10	60	10-50	74.61	0.30	21.70	78.30	46.40
290		10	30	10-50	66.5	0.40	28.20	71.80	69.20	

The abbreviations in the top row of table 11 are the following: Temp=Torrefaction peak temperature, HR=heating rate, RT=residence time, PS=estimated average particle size, GY=gravimetric yield, FC=fixed carbon content, VM=volatile matter content, and HGI=Hardgrove Grindability Index. The hardwood mix is a mix of birch and oak, while the softwood mix is a mixture of pine, spruce and larch.

The particle sizes of the feedstock in the table above were converted to estimated averages to be have them be represented by numeric values instead of ranges. Ohliger provided a mass distribution of his particle sizes allowing an average 6.5 mm to be calculated. The other two papers presented the particle sizes as given in table 11. These values are converted to single numerical in values the following way:

- <10 =6.5 Using value from Ohliger
- >20=25 Assuming average = minimum + 25%
- <4=2.6 Assuming size distribution like the one given by Ohliger
- >10=12.5 Assuming average = minimum + 25%
- 10-50=36 Assuming size distribution like the one given by Ohliger

Although not included in table 11, the ultimate analysis is available and included in the following PCA. It contains values for carbon, hydrogen and oxygen, the latter calculated as a difference. Other elements like, nitrogen and sulphur, collectively constitutes >1% of all the samples, so their values are omitted. Naturally, several of these values correlate highly with each other. For instance, fixed carbon content is associated with a proportional decrease in volatile matter given how they are defined and measured, and a comparatively low ash content. The same goes for gravimetric yield and fixed carbon content, as the mass lost through torrefaction is volatile matter. A correlation matrix is constructed of Pearson correlations where the ones with absolute value ≥ 0.4 are in bold.

Principal component analysis grindability

A PCA is now performed on the values in table 11. Because not all variables have the same units, the PCA is based on the correlation matrix, rather than the covariance matrix. The correlation matrix is given in table 12, where correlations ≥ 0.4 are in bold.

Table 12: Pearson correlation matrix

	Temp	RT	PS	GY	ASH	FC	VM	C	H	Ox	HGI
Temp	1	-0.04	0.04	-0.8	0.148	0.808	-0.81	0.731	-0.46	-0.7	0.78
RT	-0.04	1	0.003	-0.29	0.059	0.144	-0.14	0.285	-0.26	-0.29	0.146
PS	0.04	0.003	1	-0.3	-0.04	0.096	-0.02	0.17	-0.13	-0.02	0.206
GY	-0.80	-0.29	-0.3	1	-0.25	-0.91	0.885	-0.92	0.703	0.82	-0.88
ASH	0.15	0.059	-0.04	-0.25	1	0.388	-0.43	0.447	-0.54	-0.46	0.005
FC	0.81	0.144	0.096	-0.91	0.388	1	-0.99	0.89	-0.78	-0.82	0.826
VM	-0.81	-0.14	-0.02	0.885	-0.43	-0.99	1	-0.88	0.784	0.822	-0.8
C	0.73	0.285	0.17	-0.92	0.447	0.89	-0.88	1	-0.78	-0.95	0.809
H	-0.46	-0.26	-0.13	0.703	-0.54	-0.78	0.784	-0.78	1	0.689	-0.59
Ox	-0.70	-0.29	-0.02	0.82	-0.46	-0.82	0.822	-0.95	0.689	1	-0.72
HGI	0.78	0.146	0.206	-0.88	0.005	0.826	-0.8	0.809	-0.59	-0.72	1

Table 13: Importance of principal components

Importance of components:	Comp.1	Comp.2	Comp.3
Standard deviation	2.616	1.129	1.039
Proportion of Variance	0.622	0.116	0.098
Cumulative Proportion	0.622	0.738	0.836

Tables 13 and 14 display, respectively, the importance of, and the loadings of the variables on first three principal components resulting from the PCA. The data expressed in terms of these retain enough information to explain 83.6% of the variance of the data. This is indicative of a high correlation within the variables which is also evident from table 12. Components 4 through 11 have standard deviations <1, and therefore eigenvalues <1. This makes them not satisfy the Kaiser criterion for inclusion.

Table 14: Loadings of variables on principal components

<u>Loadings:</u>	Comp.1	Comp.2	Comp.3
Temp	0.312	0.261	0.314
RT		-0.257	-0.726
PS		0.424	-0.544
GY	-0.364	-0.174	0.127
ASH	0.160	-0.666	
FC	0.370		0.110
VM	-0.367		-0.156
C	0.370		
H	-0.311	0.260	0.120
Ox	-0.346	0.135	
HGI	0.329	0.350	

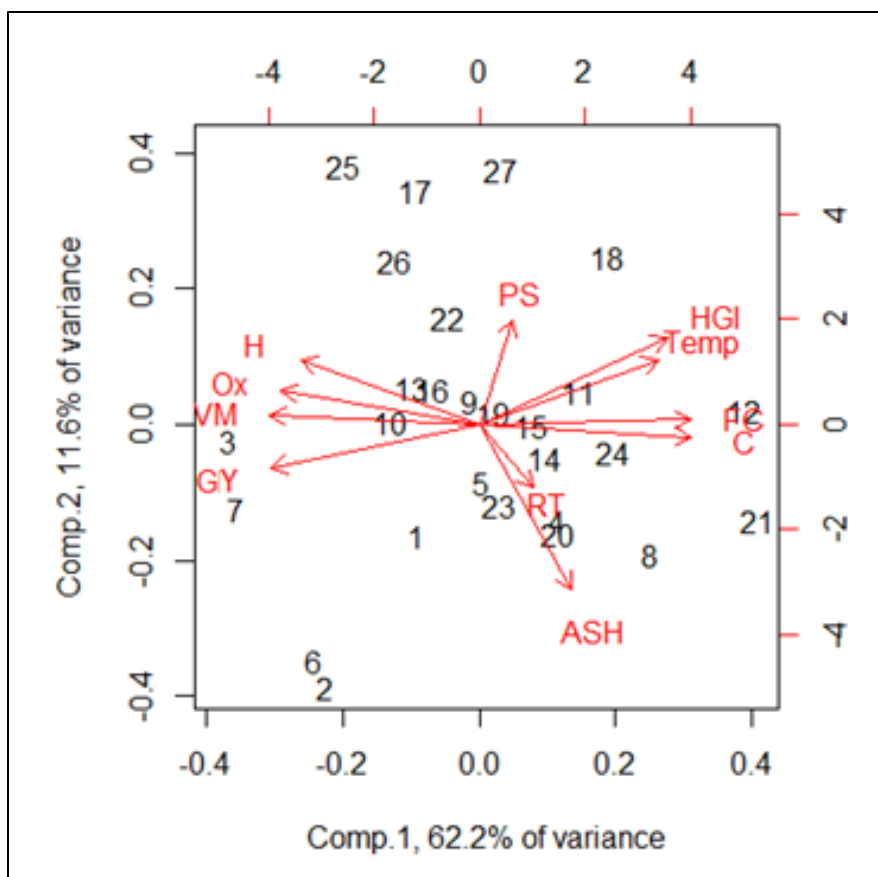


Figure 27: Biplot

Of the experimental parameters, temperature, residence time, heating rate and particle size, only temperature correlates significantly with HGI across all the samples evidenced by a Pearson correlation coefficient of 0.78 and good alignment in the biplot. However, the temperature ranks only fourth in its correlation with HGI, as GY, FC and C, in decreasing order, correlate more strongly with HGI. As opposed to in the biplot for the charcoal (figure 20), this biplot has the measure for mechanical strength (HGI) align well with temperature, fixed carbon content and gravimetric yield. These thus appear to be the relevant correlates, which also could be seen from table 12.

The projections of PS and RT in relation to HGI in figure 27 imply that these variables were not influential in determining HGI. The effect of them combined may still be a factor since the effect of one should depend on the value of the other. For a piece of wood to be thoroughly torrefied, residence time must be sufficiently long in relation to the particle size and the torrefaction temperature. To test if some of the variation in HGI is due to the wood not being completely torrefied, the value Residence time divided by particle size was calculated for each

sample. A sufficiently low value for this ratio, especially if the temperature is also low, should cause the core of the particle to be left un-torrefied, which would result in a lower HGI.

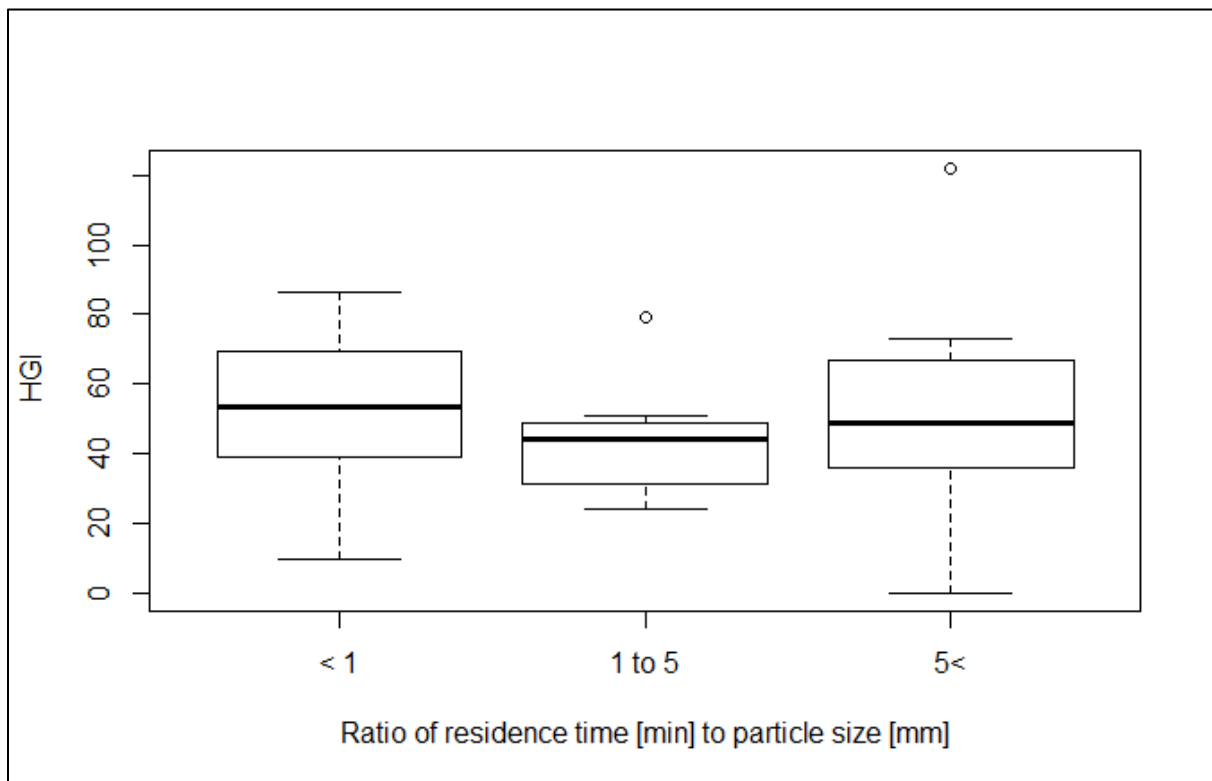


Figure 28: HGI for three ranges of RT/PS. For boxes left to right: $n=10$, $n=8$, $n=9$

There is no significant difference between the means in figure 28. This is evidence that the residence times and particle sizes were sufficiently long and small respectively, to allow complete torrefaction of the particle.

Plots of HGI and strongest correlates

To determine the effect of the different biomass types on grindability, HGI has been plotted against the three strongest correlates temperature, gravimetric yield and fixed carbon content, along with the respective regression line. In the plot against temperature (figure 29), regular linear regression is used since temperature is an independent variable. In the two other plots (figures 31 and 33), Deming regression, or orthogonal regression, is used since HGI, gravimetric yield and fixed carbon content are all measured values, and thus prone to error. The regressions yielded the following equations.

$$HGI = -293.9 + 1.24 \cdot T \text{ (figure 29)}$$

$$HGI = 224.2 - 2.46 \cdot GY \text{ (figure 31)}$$

$$HGI = -86.80 + 4.82 \cdot FC \text{ (figure 33)}$$

where T=Torrefaction temperature, GY=Gravimetric yield and FC =Fixed carbon content

To ascertain the performance of the different biomass types in relation to the regression lines, the vertical distances from the data points to the regression lines are sorted by biomass type and presented in boxplots. This gives an indication of the under- or over prediction of the regression line compared to the measured HGI values. A positive value in the boxplot indicates that the biomass was more easily grindable than suggested by the respective parameter.

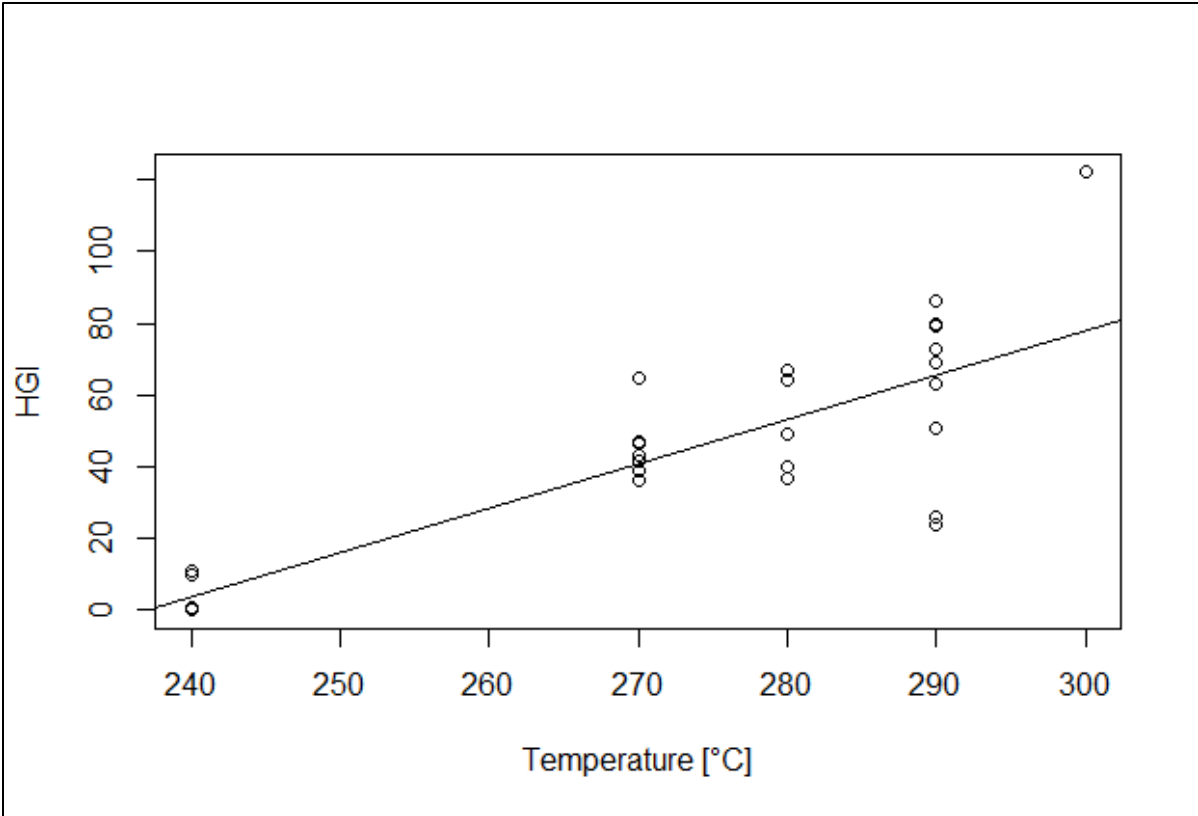


Figure 29: HGI vs temperature

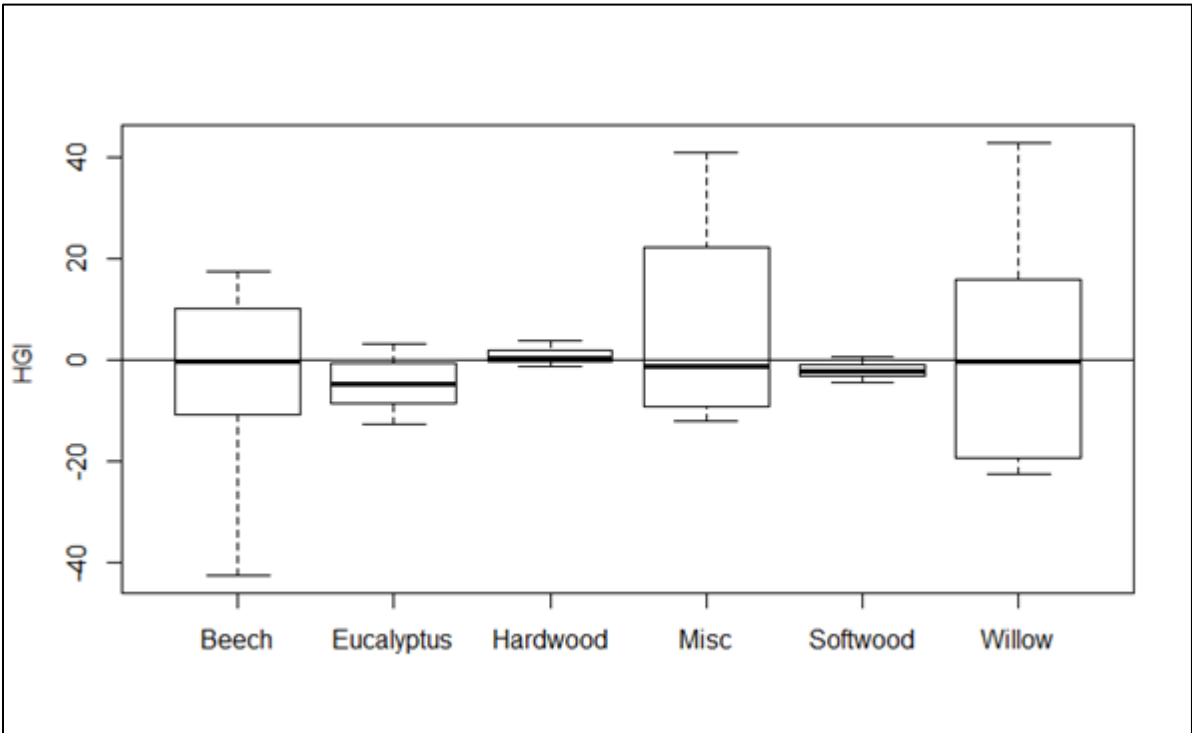


Figure 30: Deviation temperature regression line for each biomass type. Boxes from left to right: n=8, n=3, n=3, n=4, n=3, n=6.

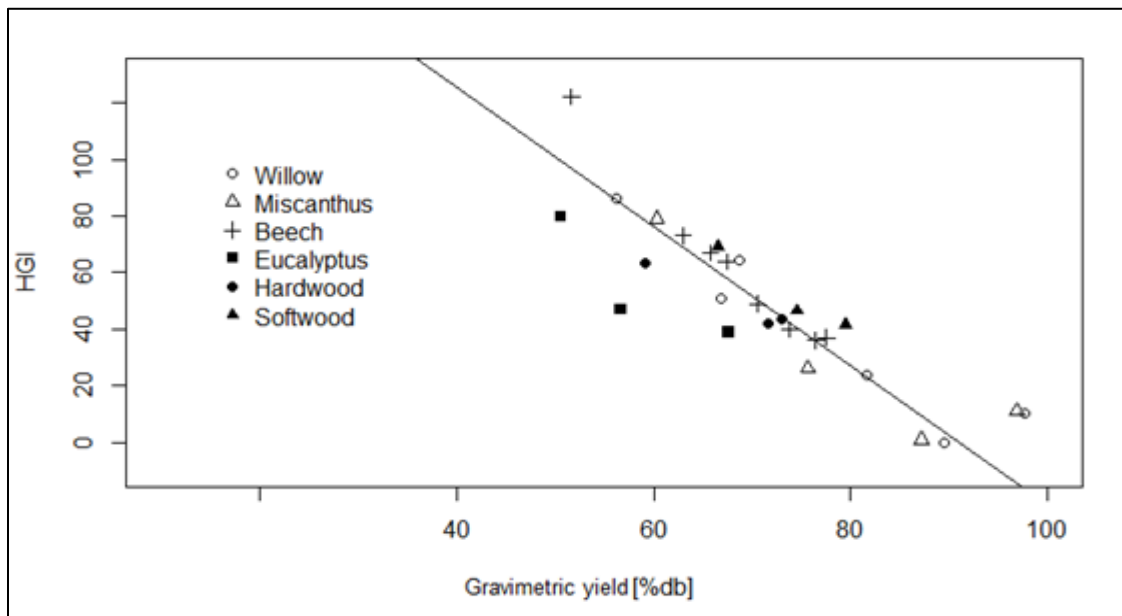


Figure 31: HGI vs gravimetric yield

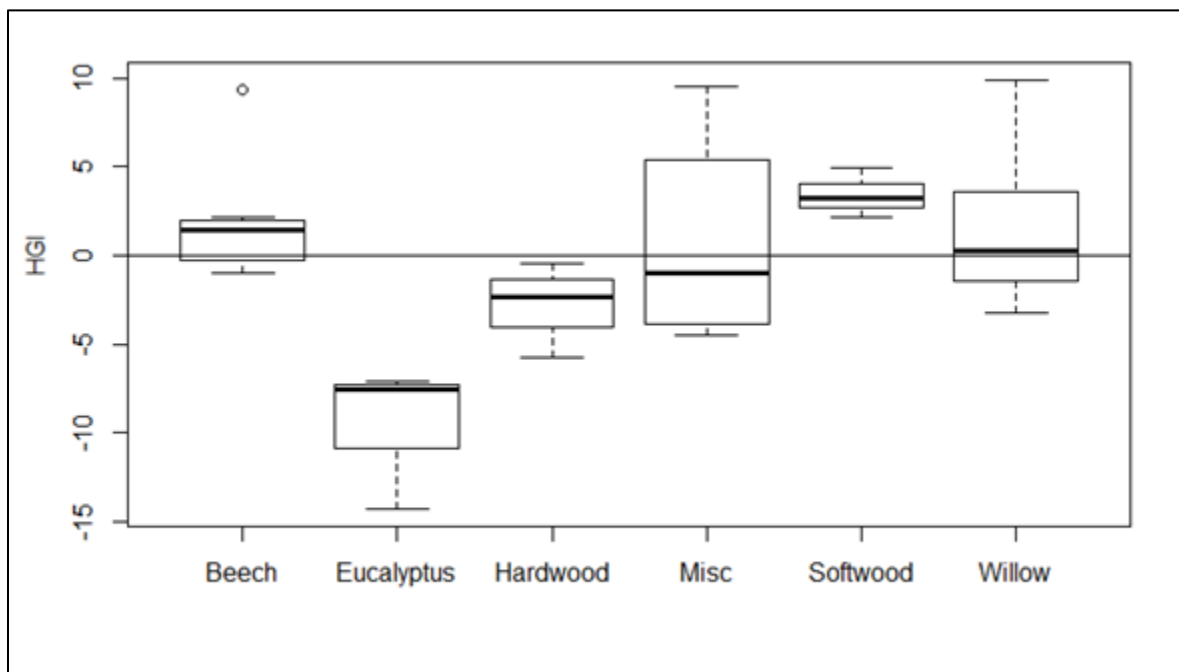


Figure 32: Deviation from gravimetric yield regression line for each biomass type. Boxes from left to right: $n=8$, $n=3$, $n=3$, $n=4$, $n=3$, $n=6$.

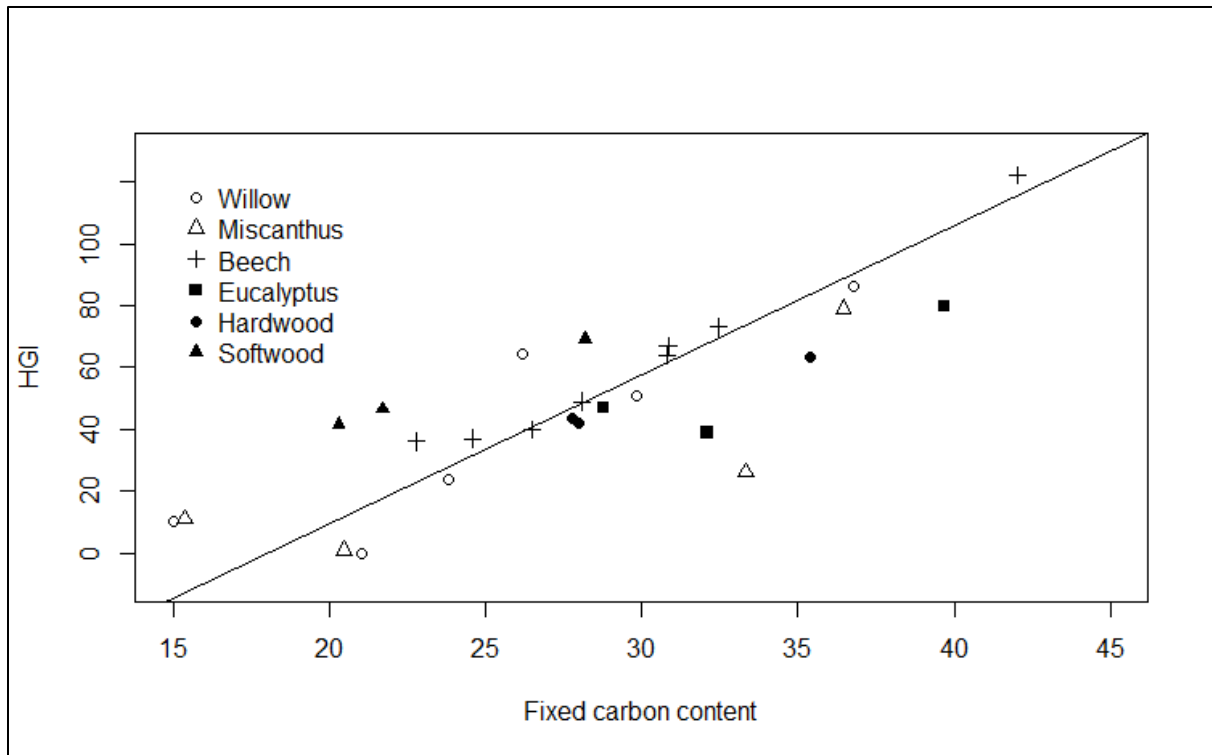


Figure 33: HGI vs fixed carbon content

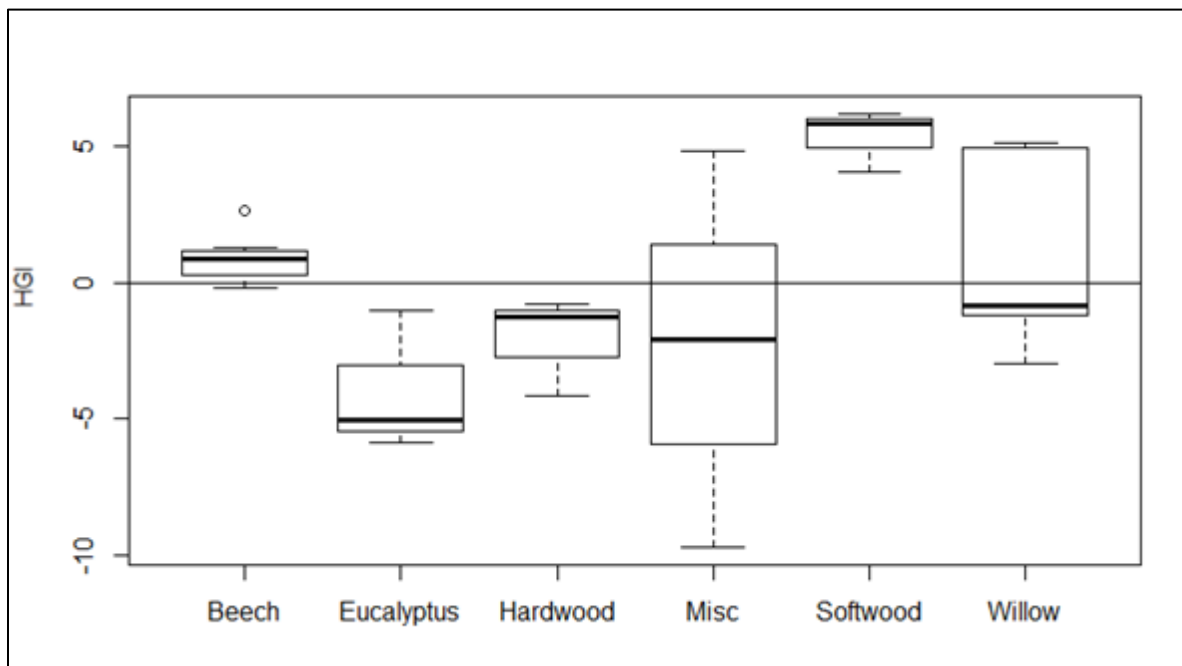


Figure 34: Deviation from fixed carbon content regression line for each biomass type. Boxes from left to right: $n=8$, $n=3$, $n=3$, $n=4$, $n=3$, $n=6$.

There appears to be no significant difference in the effect of temperature on the HGI for the different biomass species. The results from figures 31 through 34 indicate that there is a difference between species in their HGI values relative to their values for gravimetric yield and fixed carbon content. In both cases eucalyptus appears to be the hardest of the species, its HGI being overpredicted by gravimetric yield and fixed carbon content. Softwoods, on the other hand, seem significantly softer than both the gravimetric yield and fixed carbon content would dictate. The HGI values of the beech samples are well aligned with the regression line in figure 32, except for one notable outlier. In figure 34, this same sample is more in line with the rest of the samples of its respective species. The sample in question was treated at the uniquely high temperature of 300°C. This temperature is high enough to be considered outside the torrefaction zone by some (Antal and Grønli, 2003). This temperature may have been high enough for some cellulose to start decomposing, causing the apparent drop in gravimetric yield. The observation that fixed carbon content does not seem to have a corresponding increase, may be evidence that less fixed carbon is generated from cellulose than for hemicellulose. The densities of the wood were not given in the sources, neither before nor after torrefaction. Softwoods are however known to be less dense than hardwoods on average, so density may be linked to HGI. Beech and Eucalyptus have comparable high dry densities (0.6-0.7 g cm⁻³)(Noumi et al., 2014; United States Department of Agriculture, 2010), but tropical species like *Eucalyptus* ssp. tend to be diffuse porous whereas temperate hardwoods are mostly ring porous (United States Department of Agriculture, 2010). Ring-porous wood have a concentrated low density region in each growth ring which may result in a higher measured grindability when compared to equally dense diffuse-porous wood.

Conclusions

Since the relevant laboratory where experiments would have been conducted was closed during the work on this project, the data to be analysed had to be collected from the literature, which turned out to be relatively sparse. Comparison of data from different sources proved challenging for tumbler drum test, since a common standard was not strictly followed, and sample sizes were small. Additionally, the low number of variables, and the narrow range in which they varied, made the analysis and comparisons challenging.

In the range 300-700°C, temperature appears to have a small, but significant effect (p-value=0.0497) on the friability of *E. grandis* charcoal. The effect suggests that the friability at 500°C is higher than both 300 and 700°, while the temperature had the inverse effect on apparent density. Internally heated charcoal kilns in industrial charcoal production commonly have peak temperatures around 450-500°. These could thus benefit, in terms of friability, from either an increase or a decrease in temperature. In addition, an increased temperature would also increase fixed carbon content, and likely compressive strength and density, which are all desirable effects.

Wood moisture content and tree age/size had the most significant effect (p-values <0.0001) on the friability of *E. grandis* in the above temperature range and for tree ages 6-10 yrs and moisture contents from 14 to 47%. Drier wood from younger/smaller trees appeared to produce less friable charcoal. Fixed carbon content is a decent indicator of mechanical strength in the torrefaction zone (200-300°C), while in the carbonization zone (>300°C) it is not. Gravimetric yield proved the best indicator of HGI for torrefied biomass, and *Eucalyptus* sp. had the highest HGI value in relation to both its gravimetric yield and fixed carbon content, while softwoods had the lowest. Based on this, short rotation (<6 years) dense hardwood dried to <15% moisture content prior to carbonization, and carbonized at 700°C, or perhaps higher, appears to yield the most mechanically durable wood charcoal.

For future work, systematic testing like that done by de Oliveira et al., (1982c) could be done for other wood species and perhaps with additional variables, like heating rate. The findings could then possibly be verified and generalized to apply to for instance temperate

softwoods. This could help improve the quality of locally produced charcoal for metallurgical industries located where Eucalyptus does not grow, but other wood resources are plentiful, and thus relieve the pressure on tropical rainforests.

References

- Abdel-Maksoud, G., and El-Amin, A.-R. (2011). A Review on the Materials Used During The Mummification Processes in Antient Egypt. *Mediterr. Archaeol. Archaeom.* 11, 129–150.
- ABNT (1985). NBR 8740.
- Antal, M. J., and Grønli, M. (2003). The Art, Science, and Technology of Charcoal Production. *Ind. Eng. Chem. Res.* 42, 1619–1640. doi:10.1021/ie0207919.
- Antal, M. J., and Mok, W. S. L. (1990). Review of Methods for Improving the Yield of Charcoal from Biomass. *Energy and Fuels* 4, 0–4.
- Antal Jr, M. J., Allen, S. G., Dai, X., Shimizu, B., Tam, M. S., and Grønli, M. (2000). Attainment of the Theoretical Yield of Carbon from Biomass. *Ind. Eng. Chem. Res.* 39, 4024–4031. doi:10.1021/ie000511u.
- de Assis, C. O. (2007). Sistema de Carbonização da Madeira.
- de Assis, M. R. (2016). Mechanical and physical properties of eucalyptus charcoal from pyrolysis under different conditions.
- Augusto Horta Nogueira, and Luiz (2009). “Sustainable charcoal production in Brazil,” in *Criteria and indicators for sustainable woodfuels* (FAO), 31–45. Available at: <http://www.fao.org/docrep/012/i1321e/i1321e00.pdf>.
- Bamber, R. K. (1961). Sapwood and Heartwood. *For. Comm. New South Wales, Tech. Publ.*
- Bard, E. (2001). Extending the Calibrated Radiocarbon Record. *Science* (80-.). 292, 2443–2444. doi:10.1126/science.1058375.
- Barnett, J. R., and Jeronimidis, G. (2003). *Wood Quality and Its Biological Basis*.
- Blankenhorn, P. R., Barnes, D. P., Kline, D. E., and Murphey, W. K. (1978). Porosity and pore size distribution of black cherry carbonized in an inert atmosphere. *Wood Sci.* 11.
- Bridgeman, T. G., Jones, J. M., Williams, A., and Waldron, D. J. (2010). An investigation of the grindability of two torrefied energy crops. *Fuel* 89, 3911–3918.

doi:10.1016/j.fuel.2010.06.043.

- Coutinho, A. dos R., and Ferraz, E. S. B. (1988). Determinação da friabilidade do carvão vegetal em função do diâmetro das árvores e temperatura de carbonização. *Ipef*, 33–37. Available at: <http://www.ipef.br/publicacoes/scientia/nr38/cap05.pdf>.
- E. A. McGinnes, J., Kandeel, A., and Sxopa, P. S. (1971). Some structural changes observed in the transformation of wood into charcoal. *Wood Fiber Sci.* 3, 77–83.
- Emrich, W. (1985). Handbook of Charcoal making. *Sol. Energy R&D Eur. Community* 7. doi:10.1007/s13398-014-0173-7.2.
- FAO Forestry Department (1985). “Chapter 5. Safety precautions and environmental considerations,” in *Industrial charcoal making*.
- FAO Forestry Department (1987). “Using charcoal efficiently, Fixed carbon content,” in *Simple technologies for charcoal making* Available at: <http://www.fao.org/docrep/X5328E/x5328e00.htm#Contents>.
- Foley, G. (1986). Charcoal Making in Developing Countries. *Earthscan Tech. Rep. No. 5*.
- Food and Agriculture Organization of the United Nations (2015). FAOSTAT. Available at: <http://faostat3.fao.org/browse/F/FO/E>.
- Gaur, S., and Reed, T. B. (1995). An atlas of thermal data for biomass and other fuels. doi:papers://B3F20CA2-9ACD-4BA1-A510-19A2EC38FE78/Paper/p961.
- Gaur, S., and Reed, T. B. (1998). *Thermal Data for Natural and Synthetic Fuels*.
- George, C. W., and Susott, R. A. (1971). Effects of Ammonium Phosphate And Sulfate On The Pyrolysis and Combustion Of Ocellulose. *Eff. Br. mindfulness Interv. acute pain Exp. An Exam. Individ. Differ.* 1. doi:10.1017/CBO9781107415324.004.
- Githiomi, J. K., and Kariuki, J. G. (2010). Wood basic density of eucalyptus grandis from plantations in central rift valley, Kenya: variation with age, height level and between sapwood and heartwood. 22, 281–286.
- Gomes da Silva, M., Numazawa, S., Araujo, M. M., Nagaishi, T. Y. R., and Galvão, G. R. (2007). Carvão de resíduos de indústria madeireira de três espécies florestais

exploradas no município de Paragominas, PA. *Acta Amaz.* 37, 61–70.

doi:10.1590/S0044-59672007000100007.

Grønli, M. G. (1996). A theoretical and experimental study of the thermal degradation of biomass.

Hardgrove, R. M. (2015). ISO 5074:2015. Available at:

<https://www.iso.org/obp/ui#iso:std:iso:5074:ed-3:v1:en>.

Hjulström, B., Isaksson, S., and Hennius, A. (2006). Organic geochemical evidence for pine tar production in middle Eastern Sweden during the Roman Iron Age. *J. Archaeol. Sci.* 33, 283–294. doi:10.1016/j.jas.2005.06.017.

IPCC (2005). IPCC Special Report on Carbon Dioxide Capture and Storage. Available at:

https://www.ipcc.ch/pdf/special-reports/srccs/srccs_wholereport.pdf. Available at: https://www.ipcc.ch/pdf/special-reports/srccs/srccs_wholereport.pdf.

Kan, T., Strezov, V., and Evans, T. J. (2016). Lignocellulosic biomass pyrolysis : A review of product properties and effects of pyrolysis parameters. *Renew. Sustain. Energy Rev.* 57, 1126–1140. doi:10.1016/j.rser.2015.12.185.

Kataki, R., Chutia, R. S., Mishra, M., Bordoloi, N., and Saikia, R. (2015). “Chapter 2 – Feedstock Suitability for Thermochemical Processes,” in *Recent Advances in Thermo-Chemical Conversion of Biomass*, 31–74. doi:10.1016/B978-0-444-63289-0.00002-8.

Keita, J. D. (1987). Wood or charcoal - which is better? *Unasylva - No. 157-158* 39. Available at: <http://www.fao.org/docrep/s4550e/s4550e00.htm#Contents>.

Kristoferson, L. A., and Bokalders, V. (1987). *Renewable Energy Technologies: Their Applications in Developing Countries*. 2nd ed. Pergamon.

Kumar, M., Verma, B. B., and Gupta, R. C. (1999). Mechanical Properties of Acacia and Eucalyptus Wood Chars. *Energy Sources* 21, 675–685. doi:10.1080/00908319950014425.

Lana, G. (2012). Efeito da dimensão de toras no processo de colheita florestal e seus impactos no custo e na qualidade do carvão vegetal. 83.

doi:10.1017/CBO9781107415324.004.

- Lancelotti, C., Madella, M., Ajithprasad, P., and Petrie, C. A. (2010). Temperature , compression and fragmentation : an experimental analysis to assess the impact of taphonomic processes on charcoal preservation. *Archaeol Anthr. Sci* 2, 307–320. doi:10.1007/s12520-010-0046-8.
- Lehmann, J., and Joseph, S. (2015). *Biochar for environmental management*.
- Lehmann, J., Kern, D. C., Glaser, B., and Woods, W. I. (2007). *Amazonian Dark Earths: Origin Properties Management*. Kluwer Academic Publishers.
- Machado, J. G. M. S., Osório, E., Vilela, A. C. F., Babich, A., Senk, D., and Gudenau, H. W. (2010). Reactivity and Conversion Behaviour of Brazilian and Imported Coals, Charcoal and Blends in view of their Injection into Blast Furnaces. *steel Res. Int.* 81, 9–16. doi:10.1002/srin.200900093.
- Mackay, D. M., and Roberts, P. V. (1982). The dependence of char and carbon yield on lignocellulosic precursor composition. *Carbon N. Y.* 20, 87–94. doi:10.1016/0008-6223(82)90412-2.
- Mann, C. C. (2002). The Real Dirt on Rainforest Fertility. *Science (80-)*. 297, 920 LP-923. Available at: <http://science.sciencemag.org/content/297/5583/920.abstract>.
- Misginna, M. T., and Rajabu, H. M. (1996). Yield and Chemical Characteristics of Charcoal Produced by TLUD- ND Gasifier Cookstove Using Eucalyptus Wood as Feedstock. *Second Int. Conf. Adv. Eng. Technol.*, 187–192. Available at: news.mak.ac.ug/documents/Makfiles/aet2011/Misginna.ps.
- Misra, M. K., Ragland, K. W., and Baker, A. J. (1993). Wood Ash Composition As a Function of Furnace Temperature. 4, 103–116.
- Mohan, D., Pittman, C. U., and Steele, P. H. (2006). Pyrolysis of wood/biomass for bio-oil: A critical review. *Energy and Fuels* 20, 848–889. doi:10.1021/ef0502397.
- Monsen, B., Technology, S. M., Grnli, M., Nygaard, L., Asa, F., Tveit, H., et al. (1997). The Use of Biocarbon in Norwegian Ferroalloy Production.
- Mutch, R. W., and Philpot, C. W. (1970). Relation of Silica Content to Flammability in

Grasses. *For. Sci.* 16, 64–65.

Noumi, E. S., Blin, J., and Rousset, P. (2014). Optimization of Quality of Charcoal for Steelmaking using Statistical Analysis Approach. *5th Int. Conf. Eng. waste Biomass Valoriz.*, 1–14. doi:10.13140/2.1.4748.9285.

Noumi, E. S., Rousset, P., De Cassia Oliveira Carneiro, A., and Blin, J. (2016). Upgrading of carbon-based reductants from biomass pyrolysis under pressure. *J. Anal. Appl. Pyrolysis* 118, 278–285. doi:10.1016/j.jaap.2016.02.011.

Ohliger, A., Förster, M., and Kneer, R. (2013). Torrefaction of beechwood: A parametric study including heat of reaction and grindability. *Fuel* 104, 607–613. doi:10.1016/j.fuel.2012.06.112.

de Oliveira, J. B., Gomes, P. A., and de Almeida, M. R. (1982a). “Caracterização e otimização do processo de fabricação de carvão vegetal em fornos de alvenaria,” in *Carvão vegetal: destilação, carvoejamento, propriedades, controle de qualidade.*, 63–103.

de Oliveira, J. B., Gomes, P. A., and de Almeida, M. R. (1982b). “Estudos preliminares de normalização de testes de controle de qualidade do carvão vegetal,” in *Carvão vegetal: destilação, carvoejamento, propriedades, controle de qualidade.*, 7–39.

de Oliveira, J. B., Gomes, P. A., de Almeida, M. R., Mendes, Marcelo Guimarães Pinheiro, W., and Falconi, W. B. (1982c). *Carvão vegetal: destilação, carvoejamento, propriedades, controle de qualidade.* Fundação Centro Tecnológico de Minas Gerais.

Quicker, P., Freitas Seabra Da Rocha, S., Chipatecua, G., Meder, B., Löblich, H., and Franzen, D. (2011). Biokoks als Energieträger in metallurgischen Prozessen. *Chemie-Ingenieur-Technik* 83, 1944–1953. doi:10.1002/cite.201100094.

Radivojević, M., Rehren, T., Pernicka, E., Šljivar, D., Brauns, M., and Borić, D. (2010). On the origins of extractive metallurgy: new evidence from Europe. *J. Archaeol. Sci.* 37, 2775–2787. doi:10.1016/j.jas.2010.06.012.

Raimie H. H., I., Darvell, L. I., Jones, J. M., and Williams, A. (2013). Physicochemical characterisation of torrefied biomass. *J. Anal. Appl. Pyrolysis* 103, 21–30. doi:10.1016/j.jaap.2012.10.004.

- Raveendran, K., Ganesh, A., and Khilar, K. C. (1995). Influence of mineral matter on biomass pyrolysis characteristics. *Fuel* 74, 1812–1822. doi:10.1016/0016-2361(95)80013-8.
- Ronsse, F., Nachenius, R. W., and Prins, W. (2015). “Chapter 11 – Carbonization of Biomass,” in *Recent Advances in Thermo-Chemical Conversion of Biomass*, 293–324. doi:10.1016/B978-0-444-63289-0.00011-9.
- Rousset, P., Figueiredo, C., De Souza, M., and Quirino, W. (2011). Pressure effect on the quality of eucalyptus wood charcoal for the steel industry: A statistical analysis approach. *Fuel Process. Technol.* 92, 1890–1897. doi:10.1016/j.fuproc.2011.05.005.
- Scattolin, M. C., Bugliani, M. F., Cortés, L. I., Pereyra Domingorena, L., and Calo, M. (2010). Una máscara de cobre de tres mil años: estudios arqueometalúrgicos y comparaciones regionales. *Boletín del Mus. Chil. Arte Precolomb.* 15, 25–46. doi:10.4067/S0718-68942010000100003.
- Schenkel, Y. (1999). Modelisation des Flux Massiques et Energetiques dans la Carbonisation du Bois en Four Cornue.
- Schweingruber, F. H. (1966). *Tree rings and environment dendroecology*. Paul Haupt.
- da Silva, D. A., Almeida, V. C., Viana, L. C., Klock, U., and de Muñiz, G. I. B. (2014). Avaliação das propriedades energéticas de resíduos de madeiras tropicais com uso da espectroscopia NIR. *Floresta e Ambient.* 21, 561–568. doi:10.1590/2179-8087.043414.
- Sjöström, E. (1981). *Wood Chemistry: Fundamentals and Applications*.
- Slocum, D. H., McGinnes, E. A, J., and Beall, F. C. (1978). Charcoal yield, shrinkage, and density changes during carbonization of oak and hickory woods. *Wood Sci.* 11, 42–47.
- Standard Test Method for Chemical Analysis of Wood Charcoal (2013).
- Standard Test Method for Apparent and True Specific Gravity and Porosity of Lump Coke (2012).
- Steel Statistical Yearbook 2016 (2016). Available at: <http://www.worldsteel.org/steel-by-topic/statistics/Steel-Statistical-Yearbook-.html>.
- Suopajärvi, H., Pongrácz, E., and Fabritius, T. (2013). The potential of using biomass-based

reducing agents in the blast furnace: A review of thermochemical conversion technologies and assessments related to sustainability. *Renew. Sustain. Energy Rev.* 25, 511–528. doi:10.1016/j.rser.2013.05.005.

Tang, W. K., and Neill, W. K. (1964). Effect of Flame Retardants on Pyrolysis and Combustion of Acellulose. *J. Polym. Sci. Part C* 81, 65–81. doi:10.1002/polc.5070060109.

Terchick, A. A., Shoenberger, R. W., Perlic, B., and L.F., D. (1963). Mechanical and related properties of some eastern coals. *Am. Chem. Soc., Div. Fuel Chem.* 7.

Thomas, P. (2000). *Trees: Their Natural History*. Cambridge University Press.

United States Department of Agriculture (2010). *Wood Handbook - Wood as an Engineering Material*.

Vieira, R. D. S. (2009). Propriedades mecânicas da madeira de clones de Eucalyptus e do Carvão produzido entre 350°C e 900°C.

Wainwright, S. A., Biggs, W. D., Currey, J. D., and Gosline, J. M. (1982). *Mechanical Design in Organisms*. Princeton University Press.

Wei, W., Mellin, P., Yang, W., Wang, C., Hultgren, A., and Salman, H. (2013). Utilization of biomass for blast furnace in Sweden. 1–97.

Wertime, T. A. (1962). *The Coming of the Ages of Steel*. University of Chicago Press.